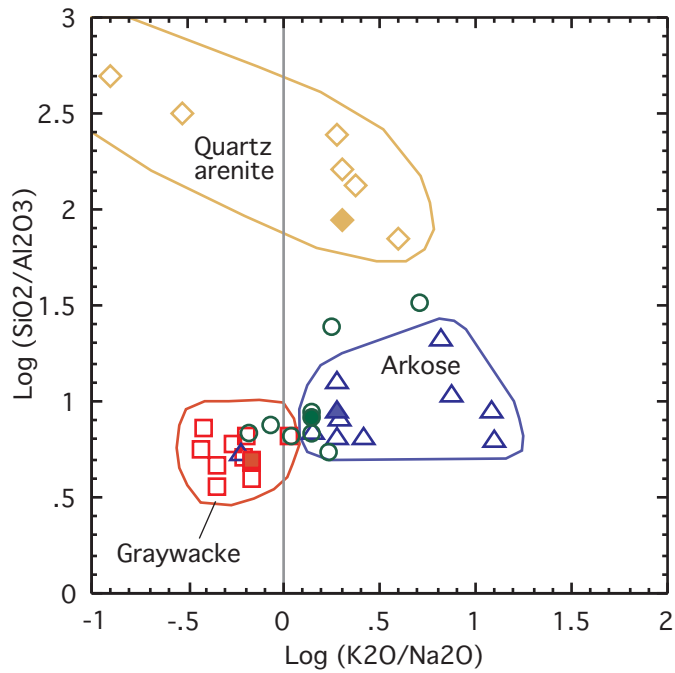


**An evaluation of alternative chemical classifications of sandstones**

by

David A. Lindsey<sup>1</sup>

**OPEN-FILE REPORT 99-346**  
**electronic edition**



**Classification of some representative sandstones (Fig. 1A)**

This report is preliminary and has not been reviewed for conformity with U. S. Geological Survey editorial standards or with the North American Stratigraphic Code. Any use of trade, product, or firm names is for descriptive purposes only and does not imply endorsement by the U. S. Government.

<sup>1</sup>U. S. Geological Survey, Denver, Colo., 80225

## CONTENTS

Summary	1
Introduction	1
Principles of classification	2
Classification of common sandstones	7
Igneous sources	9
Composition range of graywackes	12
Composition of Rocky Mountain Eocene arkoses	12
Composition of Midcontinent Pennsylvanian lithic arenites and clay-rich sandstones	18
Conclusions	21
Acknowledgments	21
References cited	21

## LIST OF FIGURES

Figure 1.—Scattergrams showing composition of representative sandstones (data from Pettijohn, 1963; 1975): A)  $\log(\text{SiO}_2/\text{Al}_2\text{O}_3)$  vs  $\log(\text{K}_2\text{O}/\text{Na}_2\text{O})$ , B)  $\log((\text{Fe}_T\text{O}_3+\text{MgO})/(\text{K}_2\text{O}+\text{Na}_2\text{O}))$  vs  $\log(\text{K}_2\text{O}/\text{Na}_2\text{O})$ , C)  $\text{SiO}_2/\text{Al}_2\text{O}_3$  vs  $\text{K}_2\text{O}/\text{Na}_2\text{O}$ , and D)  $(\text{Fe}_T\text{O}_3+\text{MgO})/(\text{K}_2\text{O}+\text{Na}_2\text{O})$  vs  $\text{K}_2\text{O}/\text{Na}_2\text{O}$ .

Figure 2.—Alternative classification diagrams showing composition of representative sandstones (data from Pettijohn, 1963; 1975): A) scattergram of  $\log(\text{Fe}_T\text{O}_3/\text{K}_2\text{O})$  vs  $\log(\text{SiO}_2/\text{Al}_2\text{O}_3)$  from Herron (1988), B) triangular scattergram of  $\text{Na}_2\text{O}-\text{K}_2\text{O}-(\text{Fe}_T\text{O}_3+\text{MgO})$  from Blatt and others (1972),

Figure 3.—Rotated three-dimensional scattergram of  $\log(\text{SiO}_2/\text{Al}_2\text{O}_3)$  vs  $\log(\text{K}_2\text{O}/\text{Na}_2\text{O})$  vs  $\log((\text{Fe}_T\text{O}_3+\text{MgO})/(\text{K}_2\text{O}+\text{Na}_2\text{O}))$  for representative sandstones (data from Pettijohn, 1963; 1975).

Figure 4.—Scattergrams showing composition of common average igneous rocks (data from Le Maitre, 1976): A)  $\log(\text{SiO}_2/\text{Al}_2\text{O}_3)$  vs  $\log(\text{K}_2\text{O}/\text{Na}_2\text{O})$ , B)  $\log((\text{Fe}_T\text{O}_3+\text{MgO})/(\text{K}_2\text{O}+\text{Na}_2\text{O}))$  vs  $\log(\text{K}_2\text{O}/\text{Na}_2\text{O})$ , C)  $\log(\text{Fe}_T\text{O}_3/\text{K}_2\text{O})$  vs  $\log(\text{SiO}_2/\text{Al}_2\text{O}_3)$ , and D) triangular scattergram  $\text{Na}_2\text{O}-\text{K}_2\text{O}-(\text{Fe}_T\text{O}_3+\text{MgO})$ .

Figure 5.—Scattergrams showing composition of tuffaceous and nontuffaceous sandstones in the Harebell Formation (data from Lindsey, 1972): A)  $\log(\text{SiO}_2/\text{Al}_2\text{O}_3)$  vs  $\log(\text{K}_2\text{O}/\text{Na}_2\text{O})$ , B)  $\log((\text{Fe}_T\text{O}_3+\text{MgO})/(\text{K}_2\text{O}+\text{Na}_2\text{O}))$  vs  $\log(\text{K}_2\text{O}/\text{Na}_2\text{O})$ , C)  $\log(\text{Fe}_T\text{O}_3/\text{K}_2\text{O})$  vs  $\log(\text{SiO}_2/\text{Al}_2\text{O}_3)$ , D)  $\log$  pct plagioclase vs  $\log(\text{SiO}_2/\text{Al}_2\text{O}_3)$ , and E) triangular scattergram  $\text{Na}_2\text{O}-\text{K}_2\text{O}-(\text{Fe}_T\text{O}_3+\text{MgO})$ .

Figure 6.—Scattergrams showing composition of graywackes and modern marine sands, classified according to plate boundary setting (data from Bhatia, 1983): A)  $\log(\text{SiO}_2/\text{Al}_2\text{O}_3)$  vs  $\log(\text{K}_2\text{O}/\text{Na}_2\text{O})$ , B)  $\log((\text{Fe}_T\text{O}_3+\text{MgO})/(\text{K}_2\text{O}+\text{Na}_2\text{O}))$  vs  $\log(\text{K}_2\text{O}/\text{Na}_2\text{O})$ , C)  $\log(\text{Fe}_T\text{O}_3/\text{K}_2\text{O})$  vs  $\log(\text{SiO}_2/\text{Al}_2\text{O}_3)$ , and D) triangular scattergram  $\text{Na}_2\text{O}-\text{K}_2\text{O}-(\text{Fe}_T\text{O}_3+\text{MgO})$ .

Figure 7.—Scattergrams showing average composition of Eocene sandstones at 36 localities in Rocky Mountain foreland basins, western United States (data from Vine and Tourtelot, 1973): A)  $\log(\text{SiO}_2/\text{Al}_2\text{O}_3)$  vs  $\log(\text{K}_2\text{O}/\text{Na}_2\text{O})$ , B)  $\log((\text{Fe}_T\text{O}_3+\text{MgO})/(\text{K}_2\text{O}+\text{Na}_2\text{O}))$  vs  $\log(\text{K}_2\text{O}/\text{Na}_2\text{O})$ , C)  $\log(\text{Fe}_T\text{O}_3/\text{K}_2\text{O})$  vs  $\log(\text{SiO}_2/\text{Al}_2\text{O}_3)$ , and D) triangular scattergram  $\text{Na}_2\text{O}-\text{K}_2\text{O}-(\text{Fe}_T\text{O}_3+\text{MgO})$ .

Figure 8.—Scattergrams showing correlations of A)  $\log(\text{SiO}_2/\text{Al}_2\text{O}_3)$  vs  $\log$  Ga ppm and B)  $\log((\text{Fe}_T\text{O}_3+\text{MgO})/(\text{K}_2\text{O}+\text{Na}_2\text{O}))$  vs  $\log$  Co ppm, average values for Eocene sandstones at 36 localities in Rocky Mountain foreland basins, western United States.

Figure 9.—Scattergram of  $\log$  cobalt ppm vs  $\log$  gallium ppm, average values for Eocene sandstones at 36 localities in Rocky Mountain foreland basins, western United States (data from Vine and Tourtelot, 1973).

Figure 10.—Scattergram of  $\log$  cobalt ppm vs  $\log$  gallium ppm for 216 samples of Eocene sandstone in Rocky Mountain foreland basins, western United States.

Figure 11.—Scattergrams showing composition of 39 analyses of Pennsylvanian sandstones from Kansas, Missouri, and Oklahoma (data from Boerngen and others, 1975): A)  $\log(\text{SiO}_2/\text{Al}_2\text{O}_3)$  vs  $\log(\text{K}_2\text{O}/\text{Na}_2\text{O})$ , B)  $\log((\text{Fe}_T\text{O}_3+\text{MgO})/(\text{K}_2\text{O}+\text{Na}_2\text{O}))$  vs  $\log(\text{K}_2\text{O}/\text{Na}_2\text{O})$ , C)  $\log(\text{Fe}_T\text{O}_3/\text{K}_2\text{O})$  vs  $\log(\text{SiO}_2/\text{Al}_2\text{O}_3)$ , and D) triangular scattergram  $\text{Na}_2\text{O}-\text{K}_2\text{O}-(\text{Fe}_T\text{O}_3+\text{MgO})$ .

Figure 12.—Variation scattergrams of 39 analyses of Pennsylvanian sandstones from Kansas, Missouri, and Oklahoma (data from Boerngen and others, 1975): A)  $\text{K}_2\text{O}$  vs  $\text{Al}_2\text{O}_3$ , B)  $\text{Na}_2\text{O}$  vs  $\text{Al}_2\text{O}_3$ , C)  $\text{K}_2\text{O}+\text{Na}_2\text{O}$  vs  $\text{Al}_2\text{O}_3$ , and D)  $\text{Al}_2\text{O}_3$  vs  $\text{SiO}_2$ .

## TABLE

Table 1.—List of analyzed sandstones compiled by Pettijohn (1963; 1975) and plotted in Figs. 1 and 2.

U.S. GEOLOGICAL SURVEY OPEN-FILE REPORT 99-346  
AN EVALUATION OF ALTERNATIVE CHEMICAL CLASSIFICATIONS OF SANDSTONES

by David A. Lindsey

### SUMMARY

Chemical classification of sandstone is worth attempting because modern analytical methods are producing extensive data sets on rock composition. Previous compilations and statistical studies have demonstrated the application of chemical data to problems in sandstone petrology, but classification has been largely ignored. Chemical data has value for classification, but the limitations of using chemical data for classification must be identified. Consideration of the processes of sandstone formation permits formulation of classification guidelines and systems for classification. Alternative systems for chemical classification can be then evaluated for their power to identify major types of sandstones and to facilitate genetic interpretation.

The relative concentrations of three major oxide groups—silica and alumina, alkali oxides, and iron oxide plus magnesia—have been used to classify sandstones. The enrichment of  $\text{SiO}_2$  by weathering and transport produces quartz arenites (orthoquartzites). Silica enrichment can be represented by  $\text{SiO}_2/\text{Al}_2\text{O}_3$ . Abundant alkalis ( $\text{Na}_2\text{O}$  and  $\text{K}_2\text{O}$ ) characterize immature sandstones such as graywackes and arkoses; the ratio  $\text{K}_2\text{O}/\text{Na}_2\text{O}$  is determined by the net effects of provenance and diagenesis. The concentration of iron oxide and  $\text{MgO}$  is the net effect of provenance and the hydraulic concentration and diagenesis of detrital ferromagnesian and iron minerals. The relative concentration of iron oxide plus magnesia can be represented by  $(\text{Fe}_T\text{O}_3+\text{MgO})/(\text{K}_2\text{O}+\text{Na}_2\text{O})$ . These ratios form the basis for chemical classification, and may be represented by two 2-dimensional diagrams or one 3-dimensional (triangular) diagram. Variants of these ratios have been used in previous classification systems.

With varying success, the classes quartz arenite, graywacke, and arkose can be defined by chemical composition. Guidelines for chemical classification are defined by plotting major oxide ratios for major classes of sandstone, and by examining compositional variation within and among the major classes. Thus, quartz arenites are here defined by  $\log(\text{SiO}_2/\text{Al}_2\text{O}_3) \geq 1.5$  and graywackes are defined by  $\log(\text{SiO}_2/\text{Al}_2\text{O}_3) < 1$  and  $\log(\text{K}_2\text{O}/\text{Na}_2\text{O}) < 0$ . Arkoses are defined by  $\log(\text{SiO}_2/\text{Al}_2\text{O}_3) < 1.5$ ,  $\log(\text{K}_2\text{O}/\text{Na}_2\text{O}) \geq 0$  and  $\log((\text{Fe}_T\text{O}_3+\text{MgO})/(\text{K}_2\text{O}+\text{Na}_2\text{O})) < 0$ . However, graywackes from passive continental margins have  $\log(\text{K}_2\text{O}/\text{Na}_2\text{O}) \geq 0$  and some arkoses have  $\log(\text{K}_2\text{O}/\text{Na}_2\text{O}) < 0$ . A fourth sandstone class, lithic arenite, is compositionally diverse; various classifications were tested with modest success, but lithic arenites cannot be identified with great confidence by chemical composition alone.

Alternative classification systems proposed previously rely on various oxide combinations, ratios, plotting methods, definitions of petrographic terms, and class boundaries. Comparison of these systems with the guidelines offered here reveals strengths and weaknesses of each. No system is ideal, and classification is facilitated by using chemical data in conjunction with petrographic data, and by exploring relationships among chemical variables that might have genetic significance.

Trace elements, notably Ga and Co, show promise for use in chemical classification. In a data set containing trace element analyses of quartzose (including lithic) arenites and arkosic sandstones, gallium is highly correlated with  $\text{SiO}_2/\text{Al}_2\text{O}_3$  and cobalt is correlated with  $(\text{Fe}_T\text{O}_3+\text{MgO})/(\text{K}_2\text{O}+\text{Na}_2\text{O})$ . Log Co vs log Ga was used to distinguish arkosic sandstones from quartz arenites, but neither could be distinguished from lithic arenites.

### INTRODUCTION

The purpose of chemical study of sandstones should not be to supplant petrographic examination, but to extend petrogenetic interpretation. However, with the introduction of modern chemical analytical methods (X-ray fluorescence, energy dispersive X-ray spectrometry, and atomic absorption spectrometry, to mention a few), large numbers of high-quality chemical analyses of rocks, including sandstones, are becoming available without corresponding detailed petrographic study. Increasingly, new down-hole analytical methods are capable of producing large numbers of analyses in a few hours (e.g., Herron and Herron, 1996). Many chemical data sets were acquired for purposes other than petrogenetic studies, such as conducting geochemical exploration for minerals, establishing geochemical baselines for environmental

studies, or identifying rocks and formations in boreholes. If rocks could be classified and interpreted from chemical data in the context of only limited petrographic data, then chemical data acquired in the course of diverse investigations could contribute to petrogenetic studies or to applications that require genetic information. For sandstones, new applications might include investigations of hydrocarbon reservoir porosity, the origin of metalliferous ore, and the effect of lithology on ground and surface water chemistry. In reality, of course, classification and interpretation from chemical data alone have severe limitations. This report is an exploration of the limits of using chemical data for classification of sandstones and an evaluation of the relative power of classification systems. For individual sandstones, the use of the classification process for insight to genetic

interpretation is illustrated.

Chemical classification of sandstone has been largely ignored by sedimentary petrographers, who preferred to classify sandstones using more accessible and definitive mineralogical and textural data derived from thin-section petrographic studies. Except for the work of Herron (1988), and brief explorations of the topic by Blatt and others (1972) and Pettijohn and others (1972), chemical studies of sandstones have been directed toward goals other than classification. Some of the first attempts to summarize and interpret chemical analyses of sandstones focused on identifying tectonic environments (Middleton, 1960; Crook, 1974; Schwab, 1975). Chemical analyses were also tabulated for representative sandstones, including those important to the naming of the common sandstone clans (called "classes" in this report) (Pettijohn, 1963; 1975; Pettijohn and others, 1972). At the time these studies were conducted, only a few hundred analyses were available in the literature, and most analyses were limited to major oxides.

Recently, trace elements and isotopes as well as major oxides have been used to investigate the origin of siliciclastic sedimentary rocks (McLennan and others, 1993). Major oxides and trace elements have been used extensively to identify graywacke provenance and correlate graywacke composition with plate-tectonic setting (Bhatia, 1983; Roser and Korsch, 1986, 1988; Floyd and others, 1991; McCann, 1991). Other studies have used geochemical data to make stratigraphic assignments (Connor, 1969; Hickman and Wright, 1983; Ehrenberg and Siring, 1992) and to identify the provenance and weathering history of sandstones (Humphreys and others, 1991; Fedo and others, 1995; Young and Nesbitt, 1998). These studies demonstrate the application of data on chemical composition to problems in sandstone petrology.

In this report, I examine some alternative methods for chemical classification of sandstones, with emphasis on the major oxide composition of the principal types of sandstone (Blatt and others, 1972; Herron, 1988; Pettijohn and others, 1972). I begin with a discussion of principles of chemical classification and various classification systems that have been proposed previously. Classification systems are compared first for a data set of representative examples of major sandstone classes; further comparisons are made through examination of data sets for each sandstone class. All of the data sets are drawn from the literature and from the work of others at the U.S. Geological Survey. Emphasis is given to graphical analysis (scattergrams and triangle diagrams) of major oxide components and simple combinations of these components that can be related to the major classes of sandstones and to processes thought to affect sandstone composition. Simple graphical methods are not a substitute for other statistical techniques, but they enable comparison of sandstone classes and depiction of general relationships among analyzed samples. Where two or

more populations are to be compared and differentiated, and where sufficient data representative of target populations are available, multivariate statistical techniques such as discriminant analysis (e.g., Connor, 1969) may be more effective than the classification techniques described here.

The approach to chemical classification of sandstones used here relies on the assumption that chemical attributes can be correlated with names assigned by petrographic study. This assumption is not always valid because, as discussed by Gilbert (in Williams and others, 1954), petrographic criteria for sandstone classification are neither consistent nor necessarily related to mineral or chemical composition. For example, "graywacke" is defined by sorting and grain size, whereas "arkose" is defined by mineral composition. "Graywacke" (or Gilbert's term, "wacke") is applied to sandstones having abundant clay- and silt-sized matrix. The composition of the sand-sized fraction varies widely. In contrast, "arkose" is applied to sandstones containing abundant feldspar. Feldspar grains in arkose include both potassic and sodic varieties, and these vary greatly in proportion. Graywacke and arkose overlap where both feldspar and matrix are abundant, as in arkosic graywacke (Williams and others, 1954), and chemical composition may not be indicative of petrographic class. A third major sandstone class, "lithic arenite," is composed of abundant sand-sized rock fragments. Lithic arenite varies in chemical composition according to the type of rock fragments. The lack of any mineralogical basis for defining graywacke and lithic arenite is a major reason for misclassification when only chemical composition is considered.

Despite the impediments to chemical classification imposed by inconsistent petrographic criteria, each sandstone class can be characterized by chemical attributes. These attributes are not unique for all classes and are best employed when petrographic observations are also available. Where chemical data alone are available, classification is improved by experimenting with alternative classification systems and by examining the data for relationships that have genetic significance.

## PRINCIPLES OF CLASSIFICATION

The concentrations of three major oxide groups have been used to classify sandstones: silica and alumina, alkali oxides, and iron oxide plus magnesia. The significance of these variables is discussed by Blatt and others (1972), Herron (1988), Pettijohn and others (1972) and, for modern river sands, Potter (1978); some important points are summarized as follows:

The enrichment of  $\text{SiO}_2$  over  $\text{Al}_2\text{O}_3$  by mechanical and chemical processes produces quartz arenites (orthoquartzites). Silica (quartz) enrichment is a measure of sandstone maturity, and is a reflection of the duration and intensity of weathering and destruction of other minerals during transport. Silica enrichment also occurs by addition of silica cement, as quartz and opal.

Abundant alkalis ( $\text{Na}_2\text{O}$  and  $\text{K}_2\text{O}$ ) characterize immature sandstones such as arkoses and graywackes. The ratio  $\text{K}_2\text{O}/\text{Na}_2\text{O}$  is determined by the sum of provenance and diagenesis. The ratio  $\text{K}_2\text{O}/\text{Na}_2\text{O}$  reflects the relative abundance of potassic feldspar and plagioclase but is also affected by the compositions of the feldspars present. Potassic feldspar commonly contains some sodium (Herron and Matteson, 1993), whereas the contribution of sodium from plagioclase is decreased by calcium substitution. The ratio  $\text{K}_2\text{O}/\text{Na}_2\text{O}$  has been used to discriminate between arkose ( $\text{K}_2\text{O} > \text{Na}_2\text{O}$ ) and graywacke ( $\text{Na}_2\text{O} > \text{K}_2\text{O}$ ) (Pettijohn, 1963). Arkoses are immature sandstones with abundant feldspar (both potassic feldspar and plagioclase). Graywackes contain abundant plagioclase (Huckenholz, 1963; Middleton, 1972). However, as will be discussed in this report, numerous exceptions to the relative abundance of  $\text{K}_2\text{O}$  and  $\text{Na}_2\text{O}$  in arkoses and graywackes have been found. Where clays, micas, and lithic fragments are present, they may also contribute significant amounts of alkalis; in particular, illite and mica contribute to the concentration of potassium.

The concentration of iron oxide ( $\text{Fe}_T\text{O}_3$ , total iron as  $\text{Fe}_2\text{O}_3$ ) and  $\text{MgO}$  is the net result of provenance and processes that concentrate and preserve detrital ferromagnesian and iron minerals (mainly amphibole, mica, illite, ilmenite, and magnetite) and their alteration products (chlorite, hematite, and some clays). Concentration of detrital ferromagnesian minerals reflects their abundance in source rocks and is increased by hydraulic sorting and is decreased by chemical destruction during weathering and diagenesis under oxidizing conditions. Studies of redbeds suggest that iron has been oxidized and redistributed locally, but not removed, during diagenesis (Walker, 1967). The low content of  $\text{MgO}$  in many arkoses stems from ferromagnesian-poor source rocks or possibly, as proposed by Blatt and others (1972, p. 318), removal during diagenesis. Based on chemical analyses of clay minerals in Herron and Matteson (1993), sandstones that contain illite or chlorite matrix would be expected to contain more iron oxide than matrix-free arenites. Abundant chloritic matrix in most graywackes accounts for the high iron oxide and  $\text{MgO}$  content of these sandstones (Pettijohn, 1963).

The three major oxide variables proposed for sandstone classification are a complex effect of provenance, sediment transport, and diagenesis. Study of major-oxide content alone cannot suffice to identify the separate effects of various processes, but the chemical composition of sandstones does bear some relationship to the action of one process or another. For example, the effects of prolonged weathering and transport are most evident in the formation of quartz arenite. Provenance is a major factor in the formation of arkose and lithic arenite. The effect of diagenesis is probably most evident in production of graywacke matrix (Cummins, 1962; Kuenen, 1966), but dissolution and cementation may be

major factors in forming quartz arenites, also.

Ratios are commonly selected for classification (e.g., Pettijohn and others, 1972, fig. 2-11; Roser and Korsch, 1986, fig. 13). They provide some distinct advantages over percentage compositional data for classifying sandstones. Ratios can be selected to represent processes believed to have been important in sandstone genesis. Thus silica enrichment can be represented by  $\text{SiO}_2/\text{Al}_2\text{O}_3$ , the relative concentrations of alkalis can be represented by  $\text{K}_2\text{O}/\text{Na}_2\text{O}$ , and the relative concentration of iron oxide plus magnesia can be represented by  $(\text{Fe}_T\text{O}_3 + \text{MgO})/(\text{K}_2\text{O} + \text{Na}_2\text{O})$ . Ratios largely overcome complex computation problems posed by abundant calcite cement, variable content of volatile components ( $\text{CO}_2$ ,  $\text{H}_2\text{O}$ ,  $\text{Cl}$ , and  $\text{F}$ ), or other constituents that may be present in unusual amounts. Ratios have also been used to sidestep the effect of closure in geochemical data, whereby negative correlations among variables are forced by the necessity of summing percentage data to 100 (Chayes, 1960; Miesch and others, 1966). Finally, use of ratios allows plotting of incomplete analyses without recalculation, making determination of volatiles and minor constituents such as  $\text{TiO}_2$  and  $\text{MnO}$  unnecessary.

Adoption of ratios for plotting chemical analyses of sandstones does not overcome problems posed by silica, carbonate, and other, less common cements, such as albite or analcime. However, the presence of silica cement in quartz arenites, where it is most common, only enhances the value of  $\text{SiO}_2/\text{Al}_2\text{O}_3$  and does not lead to misclassifying a sandstone. Carbonate cement is common in sandstones, and where the carbonate is dolomite or ankerite, the concentrations of  $\text{MgO}$  and  $\text{FeO}$  are elevated, respectively. Because ratios involving  $\text{Mg}$  and  $\text{Fe}$  oxides will be affected if these elements are present in carbonate cement, analyses should be screened before use in chemical classification. Elevated  $\text{MgO}$  or  $\text{Fe}_T\text{O}_3$  will yield anomalously high  $(\text{Fe}_T\text{O}_3 + \text{MgO})/(\text{K}_2\text{O} + \text{Na}_2\text{O})$ , causing the sample to plot outside the compositional fields for other sandstones. The presence of abundant sodium minerals as cements may also be indicated by unusual location of the sample on ratio scattergrams. Mineralogical study is the only recourse for identifying and classifying rocks with unusual cements.

Logarithmic scales were adopted for the two-dimensional ratio scattergrams used here. Most frequency distributions of major oxide ratios, upon inspection, tend to be skewed toward low values. Also, the range of some ratios is rather large, making adoption of logarithmic scales convenient for plotting. Ratios may be converted to logarithms and plotted on linear scales, or plotted directly on logarithmic scales. For computational purposes, such as fitting lines to data, the former is convenient, but logarithmic scales permit direct reading of ratio values from scattergrams.

Scattergrams of  $\log(\text{SiO}_2/\text{Al}_2\text{O}_3)$  vs  $\log(\text{K}_2\text{O}/\text{Na}_2\text{O})$  and  $\log((\text{Fe}_T\text{O}_3 + \text{MgO})/(\text{K}_2\text{O} + \text{Na}_2\text{O}))$  vs  $\log(\text{K}_2\text{O}/\text{Na}_2\text{O})$  were adopted for use in this report (Fig. 1). The

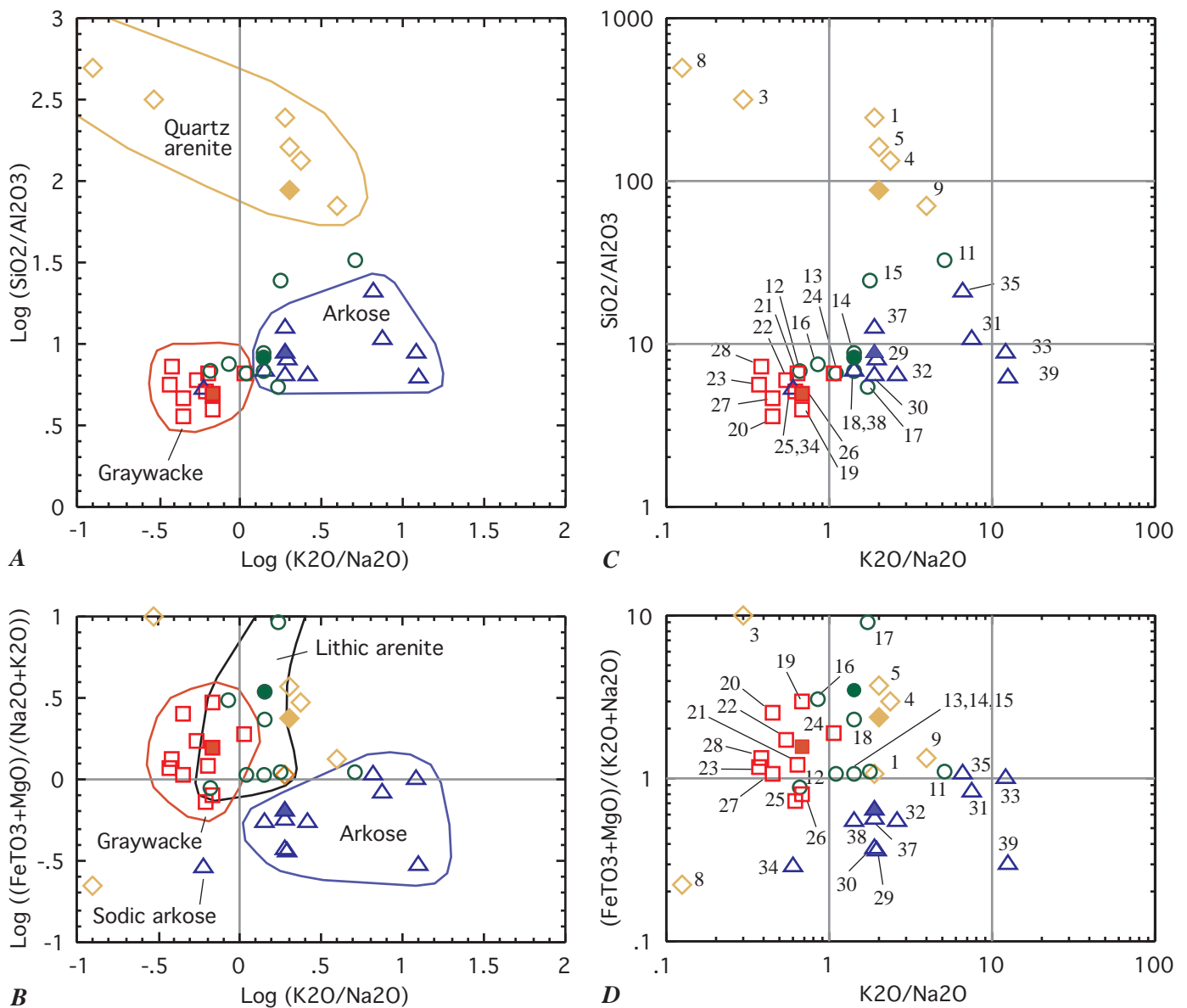


**Figure 1.**—Scattergrams showing composition of representative sandstones (data from Pettijohn, 1963; 1975): A)  $\log(\text{SiO}_2/\text{Al}_2\text{O}_3)$  vs  $\log(\text{K}_2\text{O}/\text{Na}_2\text{O})$ , B)  $\log((\text{Fe}_T\text{O}_3+\text{MgO})/(\text{K}_2\text{O}+\text{Na}_2\text{O}))$  vs  $\log(\text{K}_2\text{O}/\text{Na}_2\text{O})$ , C)  $\text{SiO}_2/\text{Al}_2\text{O}_3$  vs  $\text{K}_2\text{O}/\text{Na}_2\text{O}$ , and D)  $((\text{Fe}_T\text{O}_3+\text{MgO})/(\text{K}_2\text{O}+\text{Na}_2\text{O}))$  vs  $\text{K}_2\text{O}/\text{Na}_2\text{O}$ . A and B show ratios expressed as logarithms on a linear scale; C and D are same as A and B except raw ratios are plotted on logarithmic scales. Compositional fields for major classes of sandstones are shown in A and B. Sample numbers in C and D are identified in Table 1.

**EXPLANATION**

- ◇ Quartz arenite
- Graywacke
- △ Arkose
- Lithic arenite

Solid symbol = average

scattergram,  $\log(\text{SiO}_2/\text{Al}_2\text{O}_3)$  vs  $\log(\text{K}_2\text{O}/\text{Na}_2\text{O})$  is a variant of one first proposed by Pettijohn and others (1972, fig. 2-11), but without their overlay of compositional fields for major sandstone classes. A third possible scattergram,  $\log((\text{Fe}_T\text{O}_3+\text{MgO})/(\text{K}_2\text{O}+\text{Na}_2\text{O}))$  vs  $\log(\text{SiO}_2/\text{Al}_2\text{O}_3)$ , was investigated but appears to largely duplicate the first two. Three-dimensional scattergrams, portraying samples in terms of all three ratios, can be used to group samples and show relationships between a sample and the principal

groups. Three-dimensional scattergrams usually require rotation for optimal viewing of sample groups.

A variation of the ratio scattergrams proposed here has been used to classify terrigenous sands and shales, with application to lithologic classification from borehole geochemical logs (Herron, 1988). Herron (1988) used a scattergram of  $\log(\text{Fe}_T\text{O}_3/\text{K}_2\text{O})$  vs  $\log(\text{SiO}_2/\text{Al}_2\text{O}_3)$  to distinguish the various classes of sandstone as well as shale and other iron-rich clastic sediments (Fig. 2A). The

**Table 1.**—List of analyzed sandstones compiled by Pettijohn (1963; 1975) and plotted in Figs. 1 and 2. Geologic ages and stratigraphic nomenclature do not reflect later revisions, if any.

QUARTZ ARENITES (ORTHOQUARTZITES AND PROTOQUARTZITES)

- 1 Precambrian Mesnard Quartzite, Marquette Co., Michigan
- 2 Precambrian Lorrain Quartzite, Plummer Township, Ontario\*
- 3 Precambrian Sioux Quartzite, Sioux Falls, South Dakota
- 4 Cambrian? Lauhavuori Sandstone, Tiiliharju, Finland
- 5 Ordovician St. Peter Sandstone, Mendota, Minnesota
- 6 Ordovician Simpson Sand, Cool Creek, Oklahoma\*
- 7 Silurian Tuscarora Quartzite, Hyndman, Pennsylvania\*
- 8 Devonian Oriskany Sandstone, Berkeley Springs quarry, West Virginia
- 9 Pennsylvanian Mansfield Formation, Crawford County, Indiana
- 10 Mississippian Berea Sandstone, Berea, Ohio\*

LITHIC ARENITES (SUBGRAYWACKES AND PROTOQUARTZITES)

- 11 Jurassic Salt Wash Formation, composite of 96 samples, Colorado Plateau
- 12 Oligocene Frio Formation, composite of 10 samples, Jim Wells and Kleberg Counties, Texas
- 13 Molasse, Aquitannienne, Lausanne, Switzerland
- 14 Molasse, Granichen, Burghalde, Canton Aargau, Switzerland
- 15 Mississippian Berea Sandstone, Berea, Ohio
- 16 Molasse burdigalienne, Voreppe
- 17 Carboniferous coal measures, Westphalian coal basin, France and Belgium
- 18 Carboniferous coal measures, Westphalian coal basin, France and Belgium

GRAYWACKES

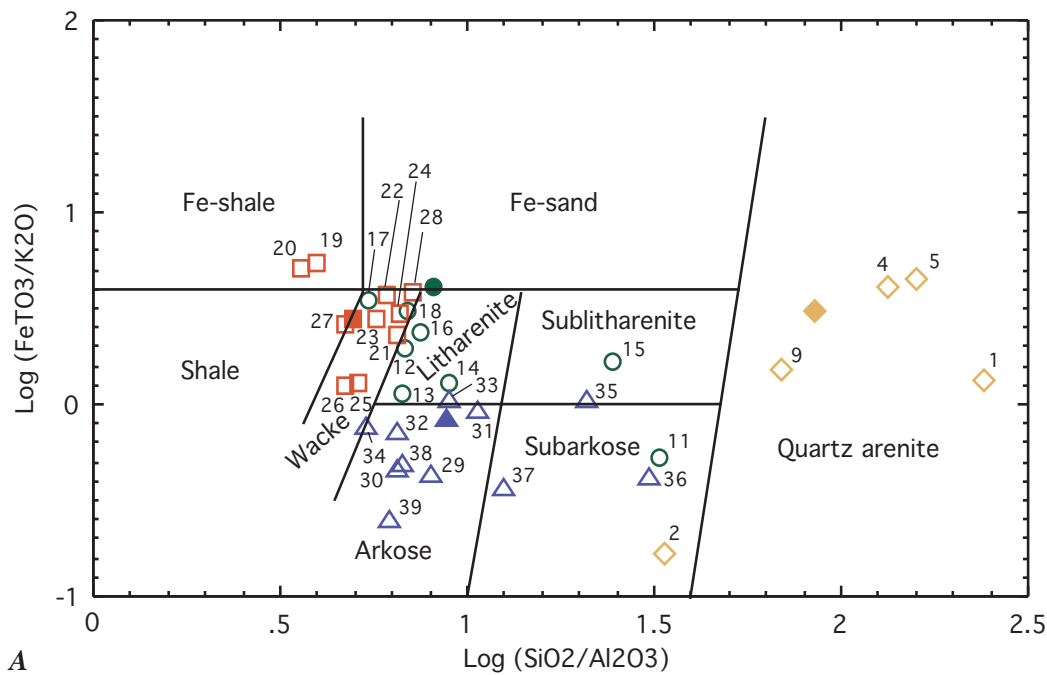
- 19 Archean, Manitou Lake, Ontario
- 20 Archean, Knife Lake, Ontario
- 21 Precambrian Tyler Slate, Hurley, Wisconsin
- 22 Ordovician? Rensselaer Graywacke, Spencertown, New York
- 23 Upper Devonian and Lower Carboniferous Tanner Graywacke, Scharzfeld, Germany
- 24 Mississippian Stanley Shale, Mena, Arkansas
- 25 Lower Mesozoic, composite of 20 graywackes, Wellington, New Zealand
- 26 Jurassic and Cretaceous Franciscan Formation, Piedmont, California
- 27 Eocene, Solduc, Washington
- 28 Carboniferous Kulm, Steinbach, Frankenwald, Germany

ARKOSES AND SUBARKOSES

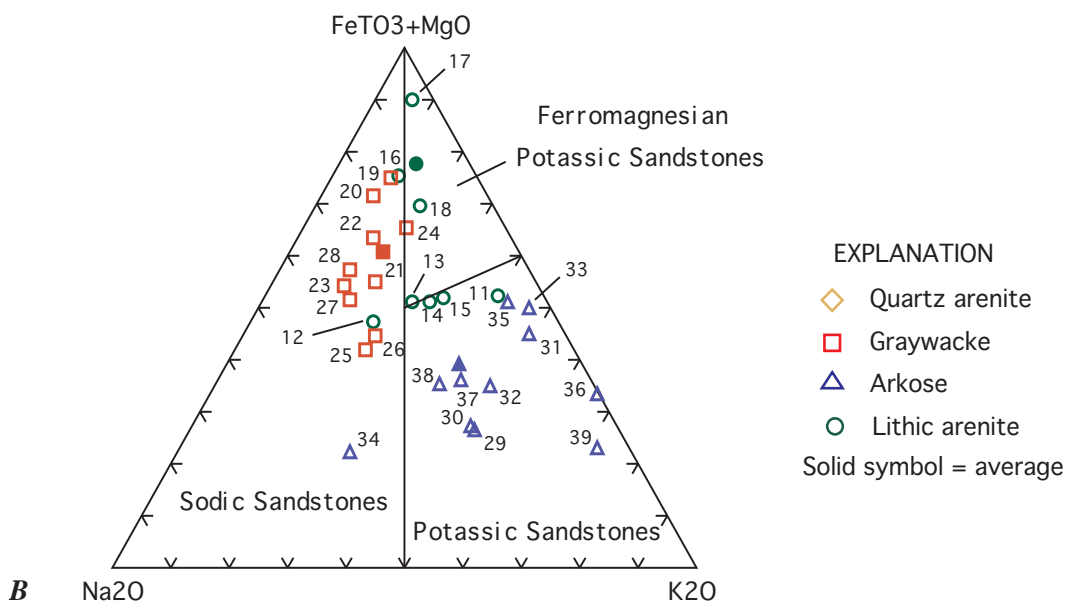
- 29 Precambrian Jotnian, Koylio, Muurunmaki, Finland
- 30 Precambrian Torridonian, Kinlock, Skye
- 31 Lower Cambrian Sparagmite, Engerdalen, Norway
- 32 Devonian lower Old Red Sandstone, Foyers, Loch Ness, Scotland
- 33 Devonian Old Red Sandstone, Red Crag, Fochabers-on-Spey, Scotland
- 34 Portland Stone (Triassic Newark Group), Portland, Connecticut
- 35 Devonian Rosebrae Sandstone, Rosebrae, Elgin, Scotland
- 36 Cambrian or Ordovician sandstone, Bastard Township, Ontario\*
- 37 Permian Whitehorse Group, Kansas
- 38 Oligocene Molasse, Unterageri, Canton Zug, Switzerland
- 39 Oligocene, Auvergne, France

\* No Na<sub>2</sub>O measurable; not included on two-dimensional ratio plots (Fig. 1)





A



B

**Figure 2.**--Alternative classification diagrams showing composition of representative sandstones (data from Pettijohn, 1963; 1975): A) scattergram of  $\log (\text{Fe}_T\text{O}_3/\text{K}_2\text{O})$  vs  $\log (\text{SiO}_2/\text{Al}_2\text{O}_3)$  from Herron (1988), and B) triangular scattergram of  $\text{Na}_2\text{O}-\text{K}_2\text{O}-(\text{Fe}_T\text{O}_3+\text{MgO})$  from Blatt and others (1972). Sample numbers are identified in Table 1.

ratio  $\log (\text{Fe}_T\text{O}_3/\text{K}_2\text{O})$  is the rough equivalent of  $\log (\text{Fe}_T\text{O}_3+\text{MgO})/(\text{K}_2\text{O}+\text{Na}_2\text{O})$ . The use of  $\text{Fe}_T\text{O}_3$  alone emphasizes concentration of iron-bearing heavy minerals such as magnetite and ilmenite in sandstone, but the omission of MgO makes the ratio less sensitive to effects of carbonate cement. Because borehole geochemical logs do not report sodium, that element was not included in the classification system of Herron (1988). The resulting classification does not take into account the ratio of  $\text{K}_2\text{O}$  to

$\text{Na}_2\text{O}$ , which may be of value for distinguishing arkoses from graywackes. Herron (1988) assigned compositional fields to each sandstone class based on a reference set of analyzed sandstones from Pettijohn (1963) and Pettijohn and others (1972), so that a name could be assigned to a sandstone by simply plotting the values of  $\log (\text{Fe}_T\text{O}_3/\text{K}_2\text{O})$  vs  $\log (\text{SiO}_2/\text{Al}_2\text{O}_3)$ . Herron's classification system is designed to distinguish subtle compositional classes such as subarkoses from arkoses and sublitharenites from

litharenites, as well as to distinguish the major sandstone classes, and it can be used with geochemical log data. Herron (1988) showed that his system provides more accurate classification of sandstones than the diagram  $\log(K_2O/Na_2O)$  vs  $\log(SiO_2/Al_2O_3)$  with compositional fields, proposed by Pettijohn and others (1972). For this reason I have used Herron's (1988) system, instead of the one by Pettijohn and others (1972), for comparison with the two-fold system  $\log(SiO_2/Al_2O_3)$  vs  $\log(K_2O/Na_2O)$  and  $\log((Fe_1O_3+MgO)/(K_2O+Na_2O))$  vs  $\log(K_2O/Na_2O)$ .

A triangular diagram (Fig. 2B) that incorporates the three components  $Na_2O$ ,  $K_2O$ , and  $(Fe_1O_3+MgO)$  represents two of the variables adopted for ratio plots (Blatt and others, 1972, p. 318). In the triangular diagram, Blatt and others (1972) do not attempt to correlate chemical composition with petrographically defined sandstone classes, but instead divide sandstones into three chemical groups: sodic sandstones, potassic sandstones, and ferromagnesian potassic sandstones. The triangular diagram is useful for classification and comparison, but relationships among samples are in some cases visually obscured by squeezing data points near the corners of the triangle. Groups of samples that should plot separately tend to merge toward one apex if one component is dominant, and mixing trends visible on two-dimensional diagrams can be obscured by scatter. On the other hand, triangular diagrams portray three components simultaneously and allow location of a sample point even when values for one or two components are zero. For the triangular diagrams of Blatt and others (1972), the three components are generally subequal in abundance and do not require multiplication or transformation to logarithms. The diagrams are employed here to compare with two-dimensional scattergrams. The two methods of plotting sandstone composition complement one another.

#### CLASSIFICATION OF COMMON SANDSTONES

Principles of classification were tested first (Figs. 1, 2 and 3) on a widely published reference set of chemical analyses of representative sandstones, tabulated by Pettijohn (1963, 1975). The set (Table 1) is only slightly larger than that used by Herron (1988); four average values for quartz arenite, arkose, graywacke, and lithic arenite (Pettijohn, 1963) are also plotted. These analyses represent classic sandstones, such as the type arkoses and graywackes, and typical examples of the major classes of sandstones. Most of the analyzed sandstones are from formations that have received independent petrographic study, and hence have been classified on that basis. For convenience, ratio scattergrams are presented both as logarithms on linear scales and as raw ratios on logarithmic scales in Figure 1.

Quartz arenites (orthoquartzites) are readily separated on the scattergram of  $\log(SiO_2/Al_2O_3)$  vs  $\log(K_2O/Na_2O)$  (Figs. 1A,C), which represents silica enrichment. Most representatives have  $\log(SiO_2/Al_2O_3) \geq 1.5$ , indicating that  $SiO_2$  is at least 30X more abundant than  $Al_2O_3$ .

Quartz arenites generally contain more than 95 percent (pct)  $SiO_2$ , or more than 90 pct quartz sand.  $\log(K_2O/Na_2O)$  varies, although most examples are potassic ( $\log > 0$ ). Four analyses of quartz arenites (Table 1) were not plotted because  $K_2O$  and  $Na_2O$  contents were so small as to be unmeasured. The scattergram of  $\log((Fe_1O_3+MgO)/(K_2O+Na_2O))$  vs  $\log(K_2O/Na_2O)$  (Figs. 1B,D) does not distinguish quartz arenites because iron oxide and magnesia values are small and erratic. As reported by Herron (1988), the scattergram of  $\log(Fe_1O_3/K_2O)$  vs  $\log(SiO_2/Al_2O_3)$  (Fig. 2A) discriminates quartz arenite well. The triangle diagram of Blatt and others (1972) (Fig. 2B) excludes sandstones having  $< 5$  pct  $Al_2O_3$  and thus, quartz arenites.

Graywackes plot in well-defined fields on all major oxide ratio diagrams (Figs. 1, 2 and 3). Generally, graywackes in the reference set plot on the  $Na_2O > K_2O$  side of the diagrams; they are characterized by fairly low  $\log(SiO_2/Al_2O_3)$  values of 0.5 to 1.0 (Fig. 1A); and they have  $\log((Fe_1O_3+MgO)/(K_2O+Na_2O))$  values between -0.2 and 0.5 (Fig. 1B). These values are close to, but not quite, in the range of average igneous rocks (Le Maitre, 1976) (Fig. 4). This near coincidence of values is not surprising, considering that many of the graywackes tabulated by Pettijohn (1963) were deposited in plate-margin environments where igneous provenance was dominant (for examples, see Roser and Korsch, 1986; Floyd and others, 1991). The slightly higher  $\log(SiO_2/Al_2O_3)$  values of graywackes compared to average igneous rocks indicate the effects of limited exposure already to the sedimentary processes of weathering and transport. The field of graywackes (labeled "wacke" in Fig. 2A) is small relative to other classes of sandstone on the scattergram of  $\log(Fe_1O_3/K_2O)$  vs  $\log(SiO_2/Al_2O_3)$ ; most graywackes, except two iron-rich Archean examples, are properly classified (Fig. 2A). Most graywackes plot to the left of the  $Na_2O = K_2O$  line in the triangle diagram of Blatt and others (1972) (Fig. 2B).

Arkoses are readily distinguished on all major oxide ratio diagrams (Figs. 1, 2 and 3). Arkoses (including subarkose) are distinguished on Fig. 1A by their generally low  $\log(SiO_2/Al_2O_3)$  of  $< 1.5$ .  $\log(SiO_2/Al_2O_3)$  values of  $< 1.3$  are common for subarkose and values  $< 1.0$  are common for arkose. A  $\log(SiO_2/Al_2O_3)$  value of 1.3 corresponds to a mixture of 75 pct quartz and 25 pct alkali (sodic or potassic) feldspar; a log value of 0.95 corresponds to a mixture of 50 pct quartz and 50 pct alkali feldspar. Generally, any rock containing 25 pct or more feldspar is considered an arkose, and rocks with 25 pct total feldspar and rock fragments (of which half is feldspar) have been called subarkose (Pettijohn, 1975). All arkoses in the reference set except one have more  $K_2O$  than  $Na_2O$ , and thus plot to the right of the line  $\log(K_2O/Na_2O) = 0$ . Values of  $\log((Fe_1O_3+MgO)/(K_2O+Na_2O))$  are generally about 0 or negative (Fig. 1B), reflecting the general paucity of ferromagnesian minerals in arkose. Arkoses are discriminated well on the scattergram log

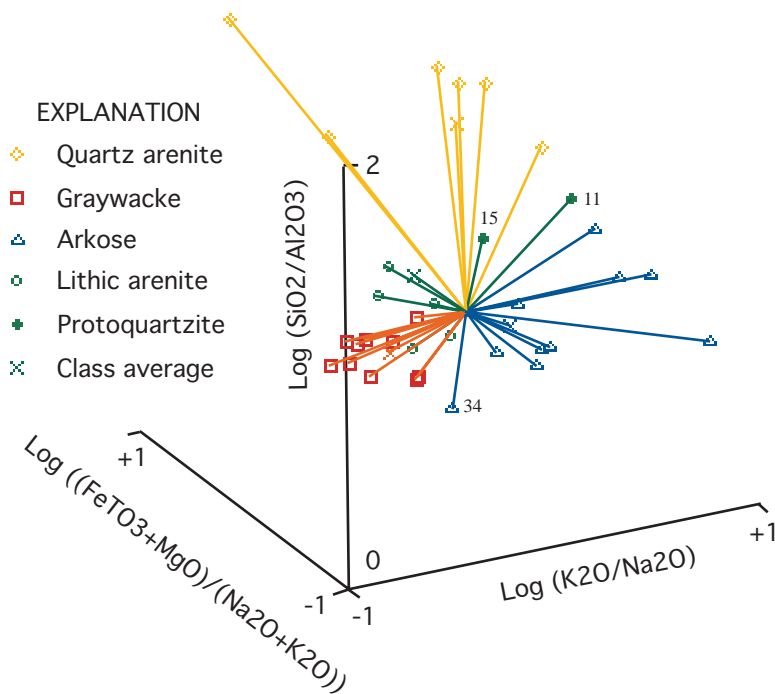


**Figure 3**—Rotated three-dimensional scattergram of  $\log (\text{SiO}_2/\text{Al}_2\text{O}_3)$  vs  $\log (\text{K}_2\text{O}/\text{Na}_2\text{O})$  vs  $\log ((\text{Fe}_T\text{O}_3+\text{MgO})/(\text{K}_2\text{O}+\text{Na}_2\text{O}))$  for representative sandstones (data from Pettijohn, 1963; 1975); individual samples are connected to the centroid of sample distribution to show sample clusters. Sample numbers are identified in Table 1.

( $\text{Fe}_T\text{O}_3/\text{K}_2\text{O}$ ) vs  $\log (\text{SiO}_2/\text{Al}_2\text{O}_3)$  of Herron (1988). Subarkoses (nos. 35, 36, and 37 on Fig. 2A) are well-separated from arkoses. Most arkoses plot to the right of the  $\text{Na}_2\text{O}=\text{K}_2\text{O}$  line and below the field of ferromagnesian potassic sandstone in the triangle diagram of Blatt and others (1972) (Fig. 2B).

One sample, of “Portland Stone” from the Hartford basin of Connecticut, plots outside the usual arkose field (no. 34, Figs. 1A,C and 2B) because it has more  $\text{Na}_2\text{O}$  than  $\text{K}_2\text{O}$ . Recent research has shown that arkoses of the Hartford basin, including the Jurassic Portland Formation, have more detrital plagioclase (mostly oligoclase) than potassic feldspar, and they also have an average 6 pct by volume albite cement (Hubert and others, 1992). The sample is properly classified in Herron’s (1988) diagram (Fig. 2A), but its sodic composition is not evident.

The class of sandstones called “lithic arenites” or “subgraywackes,” which contains more rock fragments than feldspar detritus, is not readily isolated in any of the diagrams compared here. The lithic arenites are a diverse and poorly defined class (Pettijohn, 1963). In addition to abundant rock fragments of widely varying composition, many of these sandstones contain clay matrix, and the composition of clay varies. In the scattergram of  $\log (\text{SiO}_2/\text{Al}_2\text{O}_3)$  vs  $\log (\text{K}_2\text{O}/\text{Na}_2\text{O})$ , the field of lithic arenites tends to overlap that of graywackes and arkoses, although in general the  $\log (\text{SiO}_2/\text{Al}_2\text{O}_3)$  is slightly greater for lithic arenites than for graywackes and arkoses (Fig. 1A).  $\log ((\text{Fe}_T\text{O}_3+\text{MgO})/(\text{K}_2\text{O}+\text{Na}_2\text{O}))$  vs  $\log (\text{K}_2\text{O}/\text{Na}_2\text{O})$  (Fig. 1B) discriminates between lithic arenites and arkoses but not graywackes. Herron’s (1988) diagram of  $\log (\text{Fe}_T\text{O}_3/\text{K}_2\text{O})$  vs  $\log (\text{SiO}_2/\text{Al}_2\text{O}_3)$  provides slightly better discrimination than Figs. 1A and 1B; five of eight lithic arenites plot within the fields for litharenite and

sublitharenite (Fig. 2A). However, the average litharenite of Pettijohn (1963) falls slightly outside the field of lithic arenites, and not near the center of the distribution of other lithic arenites (Fig. 2A). On the triangle diagram of Blatt and others (1972), lithic arenites tend to plot in or near the potassic ferromagnesian sandstone field, but discrimination is poor (Fig. 2B). Probably, lithic arenites cannot be identified reliably by chemical classification, even in the diagram of Herron (1988). This situation is not surprising, given that many rock fragments of lithic sandstones would be expected to vary greatly in composition.

The reference set of lithic arenites contains one sample (no. 17) with high  $\text{CO}_2$  and  $\text{MgO}$ , indicative of dolomite cement. High  $\text{MgO}$  causes sample 17 to plot in an outlying position in the scattergram  $\log ((\text{Fe}_T\text{O}_3+\text{MgO})/(\text{K}_2\text{O}+\text{Na}_2\text{O}))$  vs  $\log (\text{K}_2\text{O}/\text{Na}_2\text{O})$  (Fig. 1B) and in the triangular diagram  $\text{Na}_2\text{O}-\text{K}_2\text{O}-\text{Fe}_T\text{O}_3+\text{MgO}$  (Fig. 2B). The position of this sample is not affected by high  $\text{MgO}$  in the scatterplots  $\log (\text{SiO}_2/\text{Al}_2\text{O}_3)$  vs  $\log (\text{K}_2\text{O}/\text{Na}_2\text{O})$  (Fig. 1A) and  $\log (\text{Fe}_T\text{O}_3/\text{K}_2\text{O})$  vs  $\log (\text{SiO}_2/\text{Al}_2\text{O}_3)$  (Fig. 2A). Such sandstones can be readily identified and, if desired, removed from a sample set by searching for high  $\text{CO}_2$  (or LOI, loss on ignition) and  $\text{MgO}$  values.

Arenites intermediate in composition between quartz arenites and lithic arenites (or arkoses) are sometimes called “protoquartzites.” Protoquartzites are tabulated with both orthoquartzites and lithic arenites by Pettijohn (1963). They have less quartz than quartz arenites and generally about 90 pct  $\text{SiO}_2$ , with  $\log (\text{SiO}_2/\text{Al}_2\text{O}_3) < 1.5$ . Two examples of protoquartzites are the Jurassic Salt Wash Formation and the Mississippian Berea Sandstone (nos. 11 and 15, respectively, in Figs. 1C,D and 2). Herron (1988) reclassified the sample of Berea as subarkose, but both the mineral and chemical composition are so close to quartz

arenite that classification as subarkose vs sublitharenite is problematic. The protoquartzites are here grouped with lithic arenites. It seems likely that no chemical classification system would be capable of separating protoquartzites from other sandstone classes.

Based on study of the reference set, the following guidelines are proposed for chemical classification of sandstones:

- 1) quartz arenite:  $\log (\text{SiO}_2/\text{Al}_2\text{O}_3) \geq 1.5$
- 2) graywacke:  $\log (\text{SiO}_2/\text{Al}_2\text{O}_3) < 1$  and  $\log (\text{K}_2\text{O}/\text{Na}_2\text{O}) < 0$
- 3) arkose (includes subarkose):  $\log (\text{SiO}_2/\text{Al}_2\text{O}_3) < 1.5$  and  $\log (\text{K}_2\text{O}/\text{Na}_2\text{O}) \geq 0$  and  $\log ((\text{Fe}_T\text{O}_3+\text{MgO})/(\text{K}_2\text{O}+\text{Na}_2\text{O})) < 0$
- 4) lithic arenite (subgraywacke, includes protoquartzite):  $\log (\text{SiO}_2/\text{Al}_2\text{O}_3) < 1.5$  and either  $\log (\text{K}_2\text{O}/\text{Na}_2\text{O}) < 0$  or  $\log ((\text{Fe}_T\text{O}_3+\text{MgO})/(\text{K}_2\text{O}+\text{Na}_2\text{O})) \geq 0$ . If  $\log (\text{K}_2\text{O}/\text{Na}_2\text{O}) < 0$ , lithic arenite can be confused with graywacke.

Guidelines for chemical classification may also be expressed as fields drawn around the distribution of representative sandstones on the various diagrams (Figs. 1A,B and 2). However, these fields are more restrictive than the general guidelines offered here, and are based on the very limited number of samples in the reference set. Alternatively, sandstones can be classified using the systems of Herron (1988) or Blatt and others (1972). None of the chemical criteria or chemical classification systems employed here can be used to identify petrographic class with certainty; their use in tandem offers the best hope of assigning a rock name to an analyzed sample.

A final experiment was conducted to see if all three axes,  $\log (\text{SiO}_2/\text{Al}_2\text{O}_3)$ ,  $\log (\text{K}_2\text{O}/\text{Na}_2\text{O})$ , and  $\log ((\text{Fe}_T\text{O}_3+\text{MgO})/(\text{K}_2\text{O}+\text{Na}_2\text{O}))$ , could be used together to represent the major sandstone classes in three-dimensional space (Fig. 3). The three-dimensional scattergram was rotated for optimum separation of the four classes of sandstones, and rays were constructed from the centroid of all sample positions to the individual sample points. Although sample clusters in three-dimensional scattergrams are best visualized by spinning the axes to view a variety of perspectives, the clustering of samples is reasonably evident on certain projections in two-dimensional space (Fig. 3). Quartz arenites, arkoses, and graywackes plot in coherent clusters; lithic arenites cluster weakly, adjacent to graywackes, but some samples are indistinguishable from graywacke. The two protoquartzites of Pettijohn (1963), numbers 11 and 15, do not plot with other lithic arenites. Number 11 (Salt Wash Formation), plots between the cluster of quartz arenites and arkoses; number 15 (Berea Sandstone) most resembles the quartz arenites. The sodic arkose, number 34 ("Portland Stone"), plots between the other arkoses and the graywacke cluster. The three-dimensional method does

not successfully isolate lithic arenites, but it does isolate the other major classes of sandstones, and it is useful in establishing relationships of aberrant compositions, such as individual protoquartzites and sodic arkoses, to the major classes.

## IGNEOUS SOURCES

The presence of igneous detritus in sandstones can sometimes be identified from major oxide composition. Scattergrams of average igneous rocks (Fig. 4) define the expected compositional range of unrecycled igneous material in sandstones. In scattergrams of major oxide ratios in igneous rocks, the well-known covariation among  $\text{SiO}_2$ , alkali oxides, iron oxides, and magnesia that is generally accepted to represent magma differentiation is evident. In tuffaceous sandstones, the sedimentary processes of reworking, weathering, and mixing with non-igneous detritus are reflected by departure from the compositional range of igneous rocks. As will be illustrated, the diagrams (Fig. 4) can be used to locate the probable composition and identity of the igneous end-member in a mixing series involving an igneous source.

A simple example of mixing igneous detritus in lithic sandstones illustrates the effect on the chemical composition of sandstone, and the relative utility of the various diagrams in portraying the effects of mixing (Fig. 5). The fluvial Upper Cretaceous Harebell Formation of northwestern Wyoming contains sandstones ranging from reworked, nearly pure crystal tuff to lithic arenite and wacke with only minor amounts of volcanic detritus (Lindsey, 1972). Tuffaceous sandstones in the Harebell contain abundant volcanic quartz, a few pct potassium feldspar, abundant plagioclase (> 10 pct, typically > 20 pct), volcanic rock fragments, and biotite. Nontuffaceous sandstones contain abundant quartz with undulose extinction, only a few (< 10) pct feldspar, and both muscovite and biotite. Even in nontuffaceous sandstone, plagioclase is typically more abundant than potassium feldspar, suggesting minor mixing of tuffaceous detritus. Both sandstone classes contain as much as 28 pct nonvolcanic lithic fragments (mostly altered grains, quartzite, and chert) and both classes contain abundant clay matrix (20 pct is common). Chemical analyses of the most tuffaceous sandstones compare closely to andesite and diorite (compare Figs. 4 and 5). Chemically, nontuffaceous sandstones vary widely, but most plot in or near the litharenite field of Herron (1988) (Fig. 5C).

Alumina and soda contents are highest in tuffaceous Harebell sandstones. For tuffaceous sandstones,  $\log (\text{K}_2\text{O}/\text{Na}_2\text{O})$  is < 0; for nontuffaceous sandstones, > 0. For  $\log (\text{SiO}_2/\text{Al}_2\text{O}_3)$  vs  $\log (\text{K}_2\text{O}/\text{Na}_2\text{O})$ , both tuffaceous and nontuffaceous sandstones plot on a mixing line (Fig. 5A) that reflects varying amounts of plagioclase. In contrast, scattergrams of  $\log ((\text{Fe}_T\text{O}_3+\text{MgO})/(\text{Na}_2\text{O}+\text{K}_2\text{O}))$  vs  $\log (\text{K}_2\text{O}/\text{Na}_2\text{O})$  (Fig. 5B) and  $\log (\text{Fe}_T\text{O}_3/\text{K}_2\text{O})$  vs  $\log (\text{SiO}_2/\text{Al}_2\text{O}_3)$  (Fig. 5C) do not show the mixing line. Probably, any linear mixing trend has been disturbed by reworking

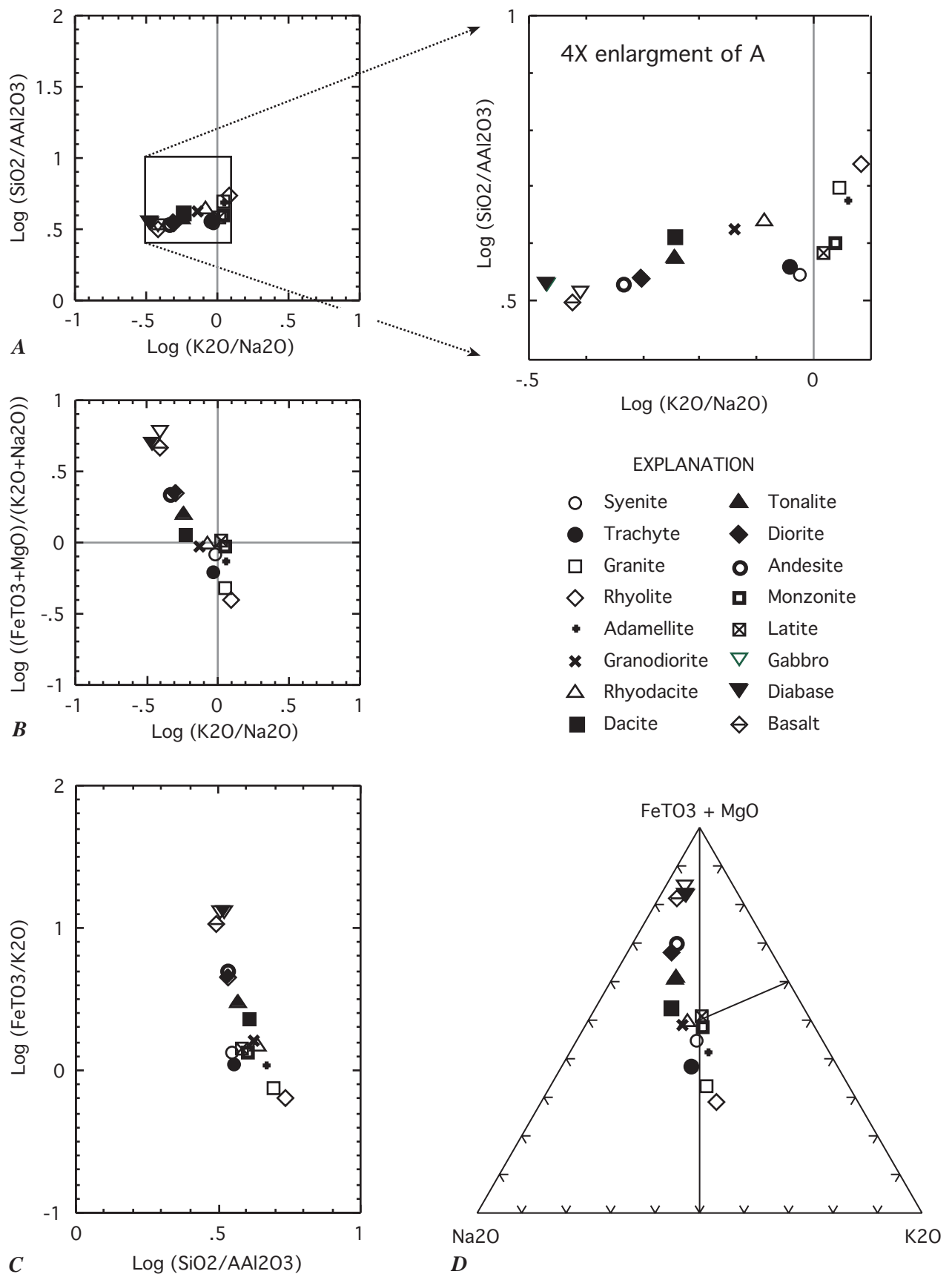


**Figure 4.**—Scattergrams showing composition of common average igneous rocks (data from Le Maitre, 1976): A) log (SiO<sub>2</sub>/Al<sub>2</sub>O<sub>3</sub>) vs log (K<sub>2</sub>O/Na<sub>2</sub>O), B) log ((Fe<sub>T</sub>O<sub>3</sub>+MgO)/(K<sub>2</sub>O+Na<sub>2</sub>O)) vs log (K<sub>2</sub>O/Na<sub>2</sub>O), C) log (Fe<sub>T</sub>O<sub>3</sub>/K<sub>2</sub>O) vs log (SiO<sub>2</sub>/Al<sub>2</sub>O<sub>3</sub>), and D) triangular scattergram Na<sub>2</sub>O-K<sub>2</sub>O-(Fe<sub>T</sub>O<sub>3</sub>+MgO).

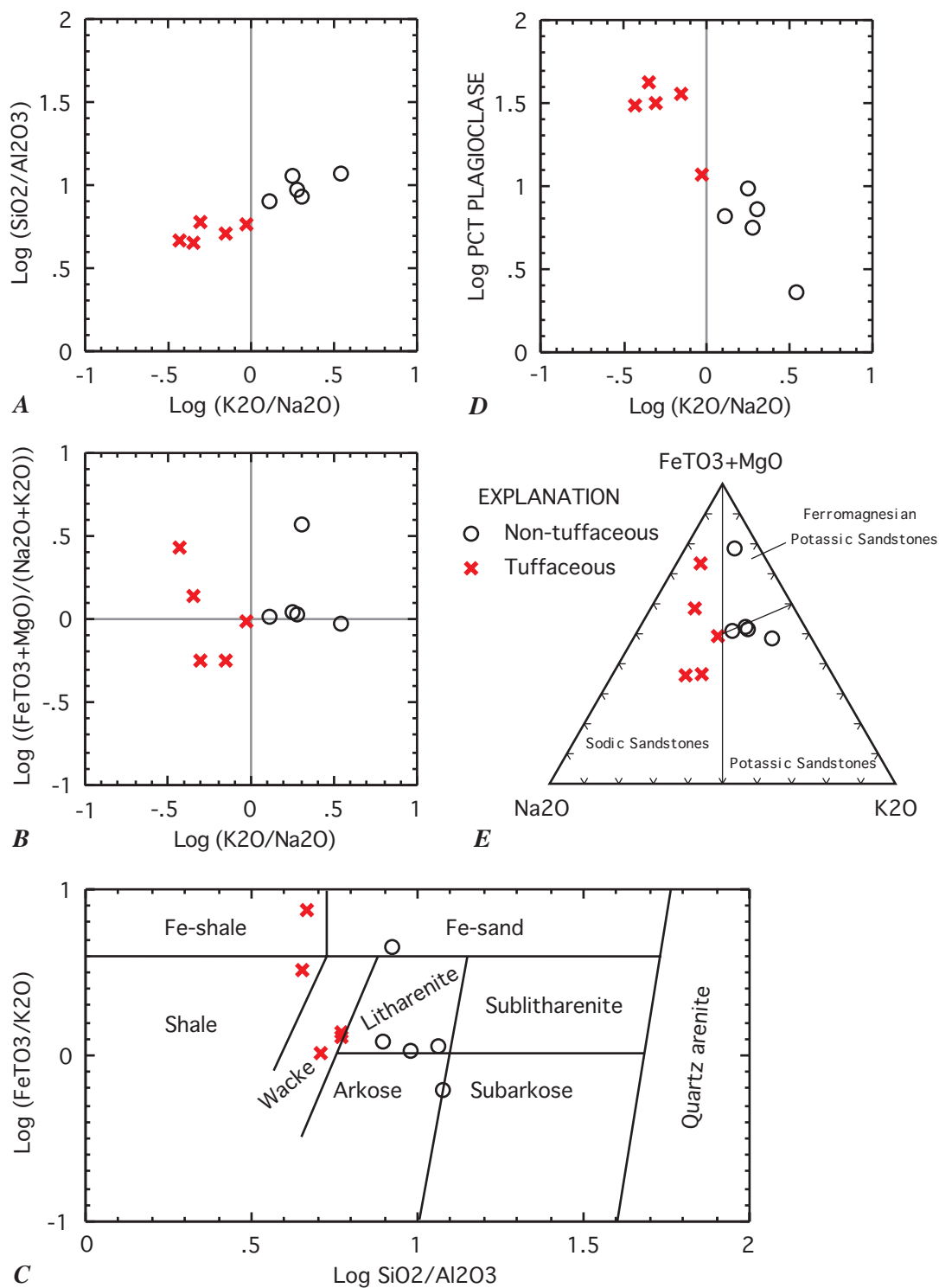


**Figure 5.**—Scattergrams showing composition of tuffaceous and nontuffaceous sandstones in the Harebell Formation (data from Lindsey, 1972): A)  $\log (\text{SiO}_2/\text{Al}_2\text{O}_3)$  vs  $\log (\text{K}_2\text{O}/\text{Na}_2\text{O})$ , B)  $\log ((\text{Fe}_T\text{O}_3+\text{MgO})/(\text{K}_2\text{O}+\text{Na}_2\text{O}))$  vs  $\log (\text{K}_2\text{O}/\text{Na}_2\text{O})$ , C)  $\log (\text{Fe}_T\text{O}_3/\text{K}_2\text{O})$  vs  $\log (\text{SiO}_2/\text{Al}_2\text{O}_3)$ , D)  $\log$  pct plagioclase vs  $\log (\text{SiO}_2/\text{Al}_2\text{O}_3)$ , and E) triangular scattergram  $\text{Na}_2\text{O}-\text{K}_2\text{O}-(\text{Fe}_T\text{O}_3+\text{MgO})$ . Classification systems in (C) and (E) from Herron (1988) and Blatt and others (1972), respectively.

and local concentration of iron oxide minerals. A scattergram of log pct plagioclase vs log ( $K_2O/Na_2O$ ) confirms the relationship between this mineral and major oxide ratios (Fig. 5D). On the triangular diagram of Blatt and others (1972), tuffaceous sandstones are discriminated from nontuffaceous sandstones of the Harebell Formation, but the mixing trend is not evident (Fig. 5E).

#### COMPOSITION RANGE OF GRAYWACKES

Graywackes represent some of the most compositionally and texturally immature sandstones, in that many of them were deposited in tectonically active plate boundary settings where erosion and sedimentation is relatively rapid. Extensive data on average graywacke compositions have been compiled and classified according to plate margin setting and compared with average modern marine sands and average composition of the major classes of sandstone (Bhatia, 1983, tabs. 5-8). These data reveal a compositional range that reflects chemical variation in provenance, ranging from igneous to sedimentary source rocks and mixtures of the two. The compositional range is correlated with four plate boundary settings: 1) oceanic island arc (= modern fore arc), 2) continental island arc (= modern back arc), 3) active continental margin (= modern leading edge), and 4) passive margin (= modern trailing edge).

Bhatia's (1983) average compositions for graywackes in various plate boundary settings are plotted here to portray the compositional range of graywackes compared to other sandstones (Figs. 6A,B). The field of Bhatia's graywackes compares well with the working definition of graywacke composition established from Pettijohn's (1963) reference data set, except that graywackes from passive continental margin settings may chemically resemble arkose and lithic arenite. Among graywackes and modern sands, log ( $SiO_2/Al_2O_3$ ) and log ( $K_2O/Na_2O$ ) increase and log ( $(Fe_T O_3 + MgO)/(Na_2O + K_2O)$ ) decreases slightly from oceanic island arc to passive margin tectonic settings.

When the compositional fields of Herron (1988) are overlaid on the scattergram log ( $Fe_T O_3/K_2O$ ) vs log ( $SiO_2/Al_2O_3$ ) (Fig. 6C), they fall far short of classifying graywackes correctly. Only seven of 22 graywackes are correctly assigned to the wacke (graywacke) field of Herron (1988). Graywackes from continental island arc and active continental margin environments overlap the wacke field, but graywackes from oceanic island arc and passive margin environments fall mostly outside the wacke field. Misclassification may result not only from the choice of oxide ratios, which excludes  $Na_2O$ , but from the choice of field boundaries and rock names. In contrast, the triangular diagram  $Na_2O-K_2O-(Fe_T O_3 + MgO)$  (Fig. 6D) discriminates most graywackes, except those from passive margins, from other sandstone classes. Comparison of Figs. 6A,B and D with C illustrates the utility of  $K_2O/Na_2O$  for distinguishing graywackes from other classes of sandstone.

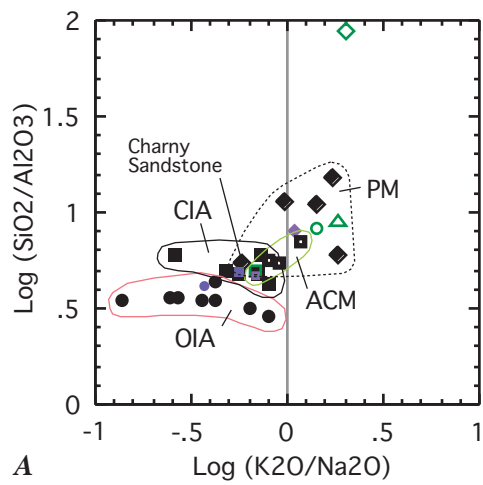
The scattergram log ( $Fe_T O_3/K_2O$ ) vs log ( $SiO_2/Al_2O_3$ ) (Fig. 6C) discriminates graywackes in some tectonic environments, particularly oceanic island arc, which is located in the field labeled "Fe-shale." Although "Fe-shale" is a misnomer for oceanic island arc graywackes, the clear separation from other tectonic environments suggests that scattergrams of log ( $Fe_T O_3/K_2O$ ) vs log ( $SiO_2/Al_2O_3$ ) may be useful in identifying oceanic island arc graywackes. For example, the two Archean graywackes of Pettijohn (1963; 1975) may represent oceanic island arc deposits (compare samples 19 and 20 in Fig. 2A with the field of OIA in Fig. 6C).

Log values of  $SiO_2/Al_2O_3$  and  $K_2O/Na_2O$  for island arc and active continental margin graywackes are comparable to those for common igneous rocks in the series basalt-rhyolite (Fig. 4A, averages from Le Maitre, 1976), but variation in the log of ( $Fe_T O_3 + MgO$ )/( $K_2O + Na_2O$ ) is less pronounced in graywackes, falling only within the range of intermediate igneous rocks (andesite - adamellite) (Fig. 4B). Thus the chemical composition of most graywackes deposited in active tectonic environments resembles that of their source rocks. In the passive margin (modern trailing edge) environment, high log ( $SiO_2/Al_2O_3$ ) and log ( $K_2O/Na_2O$ ) values for graywackes reflect prolonged or multiple cycles of weathering and transport in the sedimentary mill as well as continental sedimentary and granitic sources. The composition of graywackes deposited in passive margin environments is comparable to that of arkose and lithic arenite, suggesting that these graywackes cannot be discriminated from other classes of sandstone by chemical means.

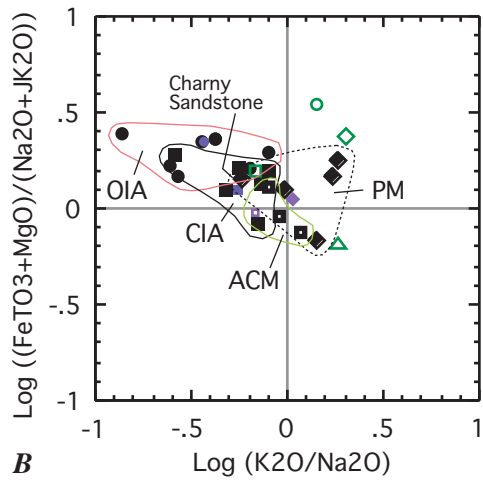
Soda metasomatism during diagenesis may have affected the composition of some graywackes. The fields for passive margin graywackes would be restricted to the  $K_2O > Na_2O$  side of scattergrams were it not for the Ordovician Charny Sandstone of Quebec (Fig. 6A,B). Soda equals or exceeds  $K_2O$  in the Charny because detrital potassium feldspar has been replaced by albite (Middleton, 1972). Albitization of feldspar has also been reported for Devonian graywackes in Europe, but chemical changes are thought to have been minimal (Floyd and others, 1991). Overall, the ratio of  $K_2O$  to  $Na_2O$  for most graywackes compared to their probable source rocks (compare Figs. 6 and 4) does not reveal the enrichment of  $Na_2O$  that might be expected if diagenetic replacement of potassium feldspar by sodium feldspar was widespread.

#### COMPOSITION OF ROCKY MOUNTAIN EOCENE ARKOSES

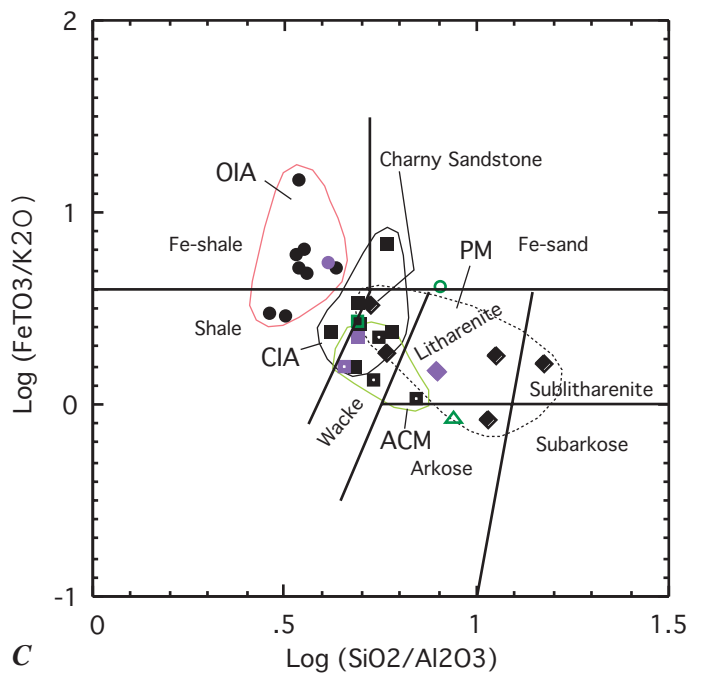
Arkose is well-represented in Laramide foreland basins of the Rocky Mountains. Sand and gravel, deposited by alluvial fans and braided to meandering streams, accumulated around basin margins (e.g., Roehler, 1993). The western sides of foreland basins immediately adjacent to the Rocky Mountain Cordilleran thrustbelt were filled with quartz and lithic detritus eroded from



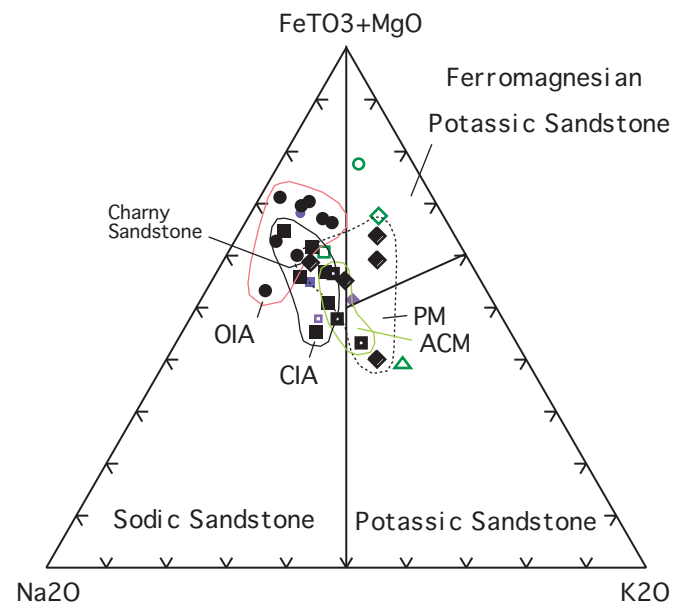
A



B



C



D

- EXPLANATION
- Oceanic Island Arc (OIA) Graywacke
  - Continental Island Arc (CIA) Graywacke
  - Active Continental Margin (ACM) Graywacke
  - ◆ Passive Margin (PM) Graywacke
  - Modern Fore-arc Sand
  - Modern Back-arc Sand
  - Modern Leading Edge Sand
  - ◆ Modern Trailing Edge Sand
  - Average Graywacke
  - △ Average Arkose
  - Average Lithic Arenite
  - ◇ Average Quartz Arenite

**Figure 6.**—Scattergrams showing composition of graywackes and modern marine sands, classified according to plate boundary setting (data from Bhatia, 1983): A)  $\log (\text{SiO}_2/\text{Al}_2\text{O}_3)$  vs  $\log (\text{K}_2\text{O}/\text{Na}_2\text{O})$ , B)  $\log ((\text{FeTO}_3+\text{MgO})/(\text{K}_2\text{O}+\text{Na}_2\text{O}))$  vs  $\log (\text{K}_2\text{O}/\text{Na}_2\text{O})$ , C)  $\log (\text{FeTO}_3/\text{K}_2\text{O})$  vs  $\log (\text{SiO}_2/\text{Al}_2\text{O}_3)$ , and D) triangular scattergram  $\text{Na}_2\text{O}-\text{K}_2\text{O}-(\text{FeTO}_3+\text{MgO})$ . Classification systems in (C) and (D) from Herron (1988) and Blatt and others (1972), respectively.



thrust sedimentary rocks, but inland from the thrustbelt, foreland basins on the craton were filled with arkosic detritus from adjacent basement-cored uplifts. The foreland basins on the craton were yoked to adjacent uplifts along thrust and reverse faults that penetrated the basement. These basins subsided from Late Cretaceous to middle Eocene time, concurrently with development of the thrustbelt (Dickinson and others, 1988).

The mineral and chemical composition of 216 samples of lower Eocene fluvial sandstone from 36 localities in the foreland basins was reported by Vine and Tourtelot (1973). These samples represent sandstones derived from sedimentary rocks of the thrustbelt (west sides of the Green River and Uinta basins) and igneous and metamorphic rocks of basement-cored uplifts (all other basins). Their composition was examined here to test chemical criteria for distinguishing arkose and to explore the compositional range of arkose.

Each locality is represented by six samples, which were analyzed for mineralogy, major oxides, and trace elements. Average (geometric mean) values were calculated to summarize the data for each locality (Vine and Tourtelot, 1973, tab. 7). The mineral content of sandstone at each locality, determined by X-ray diffraction, was plotted on a quartz-carbonate-feldspar triangular diagram (Vine and Tourtelot, 1973, fig. 3), permitting sandstones at each locality to be classified as quartzose (<10 pct feldspar), subarkose (10-25 pct feldspar), and arkose (>25 pct feldspar). Absent modal analyses of thin sections, lithic arenite cannot be distinguished with confidence. Reliance on X-ray diffraction instead of microscopic modal analysis prevents further resolution of quartzose sandstones into petrographic classes, but the X-ray data are excellent for identifying arkosic sandstones.

Major oxide ratios for the Eocene sandstone localities show good agreement with the X-ray mineralogical classification of locality averages (Fig. 7A,B). Most arkose (>25 pct feldspar) and subarkose (10-25 pct feldspar) localities plot near the arkose field defined from Pettijohn's (1963, 1975) tabulated analyses (compare Figs. 1A,B with 7A,B). However, Eocene arkoses have a broader compositional range than the arkoses tabulated by Pettijohn, especially for  $\log ((\text{Fe}_T\text{O}_3+\text{MgO})/(\text{Na}_2\text{O}+\text{K}_2\text{O}))$  vs  $\log (\text{K}_2\text{O}/\text{Na}_2\text{O})$  (Fig. 7B). Probably, the compositional range of Pettijohn's tabulated arkoses is too small; his list includes only nine examples, plus one sodic arkose (Fig. 1, Table 1). The guidelines proposed at the end of the section on classification extend the compositional range of arkose. An experiment using all three axes— $\log (\text{SiO}_2/\text{Al}_2\text{O}_3)$ ,  $\log (\text{K}_2\text{O}/\text{Na}_2\text{O})$ , and  $\log ((\text{Fe}_T\text{O}_3+\text{MgO})/(\text{Na}_2\text{O}+\text{K}_2\text{O}))$ —to examine sample clusters in three-dimensional space, yielded little information beyond that gleaned from Fig. 7.

Major oxide ratios show that sandstone at several localities (1 and 18), classified as quartzose using X-ray diffraction data, appears to be clay- or feldspar-rich; thin-section descriptions and X-ray data indicate that samples

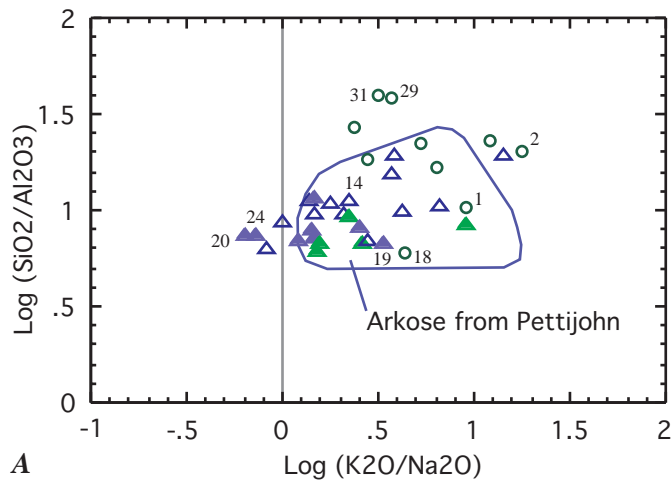
at both localities contain kaolinite and mica in addition to potassium feldspar. Locality 2, identified as having the most quartz by Vine and Tourtelot (1973), appears properly classified by major oxide ratios, but the ratios show that the most mature (silica-rich) sandstones occur at localities 29 and 31, both located near the thrustbelt in the Green River and Uinta basins, respectively. Average  $\log (\text{SiO}_2/\text{Al}_2\text{O}_3)$  values for these two localities are the only ones that fall within the quartz arenite range defined from Pettijohn's (1963, 1975) reference data set (compare Figs. 1A and 7A). Sandstones near the overthrust belt are likely to contain abundant recycled quartz and chert from thrust sedimentary rock instead of first-cycle feldspar from uplifts of Precambrian igneous and metamorphic rock.

Sandstones at five localities near the Granite Mountains of Wyoming are among the most feldspathic in the Rocky Mountain Eocene, in that they tend to have the lowest values of  $\log (\text{SiO}_2/\text{Al}_2\text{O}_3)$  and  $\log ((\text{Fe}_T\text{O}_3+\text{MgO})/(\text{Na}_2\text{O}+\text{K}_2\text{O}))$  (Fig. 7A,B). These localities are among those identified by Vine and Tourtelot (1973) as containing abundant arkose. The Granite Mountains uplift consists mainly of Precambrian granitic rock and is the likely source of arkose at localities nearby (Love, 1970).

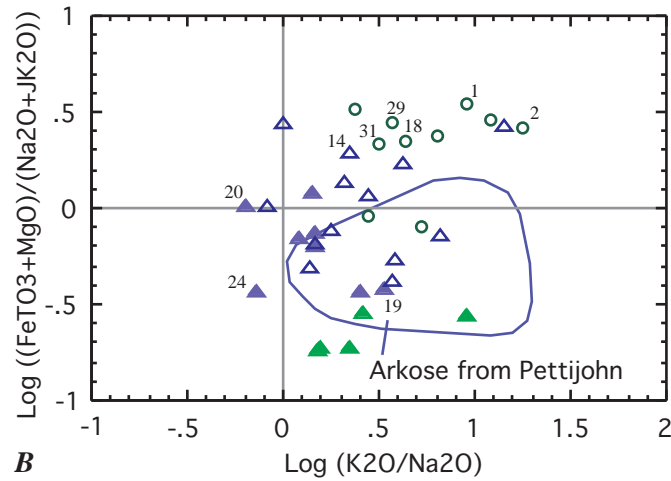
Two localities (20 and 24) having sodic arkose are identified (Figs. 7A,B). Locality 20, at West Spanish Peak in the Raton Basin, represents metamorphosed sandstone enriched in secondary prehnite, laumontite, and plagioclase (Utada and Vine, 1984). Before metamorphism by heat and fluids from the Spanish Peaks intrusions, the arkose at locality 20 was probably similar in composition to the potassic arkose of Huerfano Park (locality 19). The origin of the sodic arkose at locality 24, in the San Juan Basin, is unknown to me; arkose at locality 24 contains a large amount of plagioclase as well as potassium feldspar (Vine and Tourtelot, 1973, tab. 7).

In the classification system of Herron (1988), relying on  $\log (\text{Fe}_T\text{O}_3/\text{K}_2\text{O})$  vs  $\log (\text{SiO}_2/\text{Al}_2\text{O}_3)$ , all but one of the arkose localities falls in the field for arkose (Fig. 7C). However, thirteen localities characterized as subarkose by X-ray mineralogy are variously classified as litharenite (5), arkose (5), subarkose (2), and sublitharenite (1). None of the quartzose sandstones plot in the quartz arenite field of Herron (1988). The ten localities having quartzose sandstone defined by X-ray mineralogy are classified as sublitharenite (5), subarkose (3), litharenite (1) and wacke (1). The most quartz-rich sandstones noted by Vine and Tourtelot (1973) (nos. 1 and 2) are classified as litharenite and sublitharenite, respectively. The most quartzose sandstones defined by  $\log (\text{SiO}_2/\text{Al}_2\text{O}_3)$  (nos. 29 and 31) are classified as sublitharenite and subarkose. Sodic arkoses (nos. 20 and 24) are not separately distinguished. The sodic arkose of West Spanish Peak (no. 20) is misclassified as litharenite, albeit it is the only arkose misclassified by the system of Herron (1988).

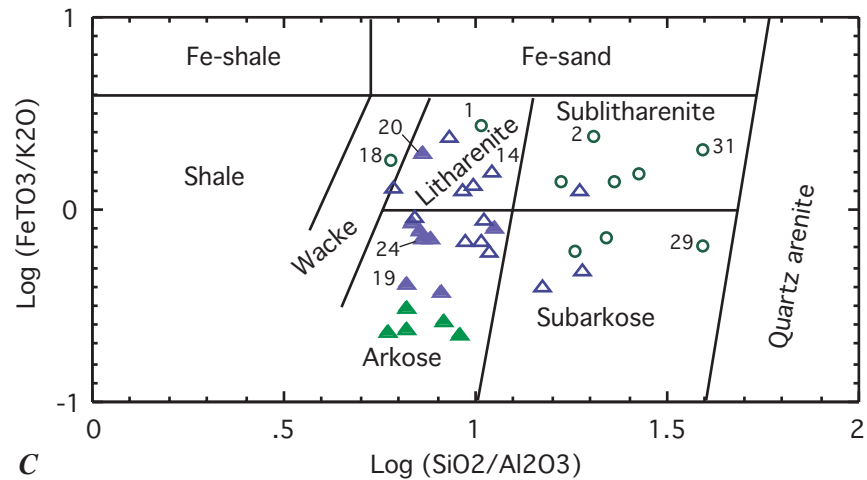
On the triangle diagram of Blatt and others (1972) (Fig. 7D), the potassic arkoses at localities surrounding the



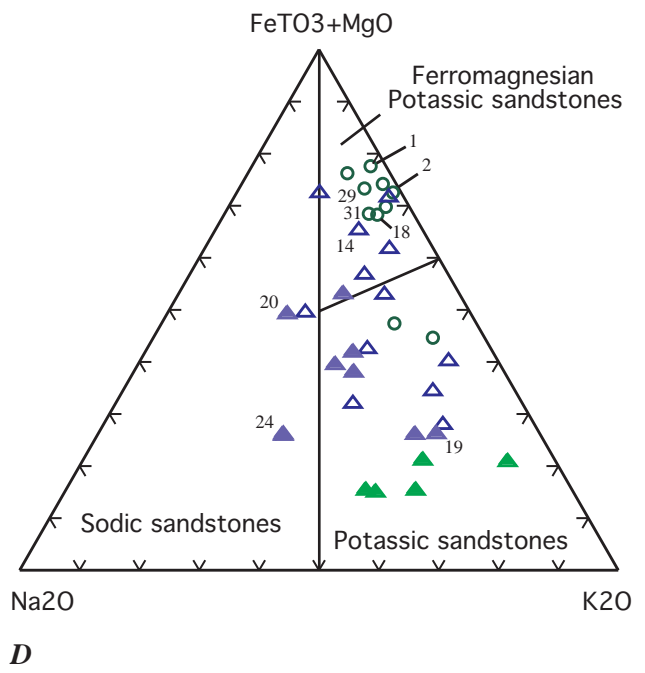
A



B



C



D

EXPLANATION

- Quartzose sandstone (< 10 pct feldspar)
- △ Subarkose (10-25 pct feldspar)
- ▲ Arkose (> 25 pct feldspar)
- ▲ Arkose (> 25 pct feldspar) near Granite Mountains

**Figure 7.**—Scattergrams showing average composition of Eocene sandstones at 36 localities in Rocky Mountain foreland basins, western United States (data from Vine and Tourtelot, 1973): A)  $\log (\text{SiO}_2/\text{Al}_2\text{O}_3)$  vs  $\log (\text{K}_2\text{O}/\text{Na}_2\text{O})$ , B)  $\log ((\text{Fe}_2\text{O}_3+\text{MgO})/(\text{K}_2\text{O}+\text{Na}_2\text{O}))$  vs  $\log (\text{K}_2\text{O}/\text{Na}_2\text{O})$ , C)  $\log (\text{Fe}_2\text{O}_3/\text{K}_2\text{O})$  vs  $\log (\text{SiO}_2/\text{Al}_2\text{O}_3)$ , and D) triangular scattergram  $\text{Na}_2\text{O}-\text{K}_2\text{O}-(\text{Fe}_2\text{O}_3+\text{MgO})$ . Classification systems in (C) and (D) from Herron (1988) and Blatt and others (1972), respectively. Localities are classified using mineral composition data of Vine and Tourtelot (1973, fig. 3). Numbered

localities are from Vine and Tourtelot (1973, tab. 1) and located therein: 1, Enos Creek, Bighorn Basin, Wyoming; 2, Hillberry Rim, Bighorn Basin, Wyoming; 14, Hoback Basin, Wyoming; 18, Horse Creek-Crazy Woman Creek, Powder River Basin, Wyoming; 19, Huerfano Park, Raton Basin, Colorado; 20, West Spanish Peak, Raton Basin, Colorado; 24, Gobernador, San Juan Basin, New Mexico; 29, Salina, Wasatch Plateau, Utah; 31, Woodruff, Wasatch Range, Utah.

Granite Mountains are plotted in a compact field closest to the  $K_2O$  apex. The sodic arkoses of localities 20 and 24 are readily separated from potassic arkose, and the difference in composition of the sodic arkose of West Spanish Peak (locality 20) and its probable potassic protolith (approximated by locality 19) is evident. The ten localities having quartzose sandstone were plotted on the triangle diagram for comparison even though eight of them contain average  $Al_2O_3$  values of  $< 5$  pct. However, eight of ten quartzose sandstone localities have  $\log(SiO_2/Al_2O_3) < 1.5$ , indicating that most quartzose sandstone is not chemical quartz arenite. The quartzose sandstone localities plot together in the field of ferromagnesian potassic sandstones. The tendency of quartzose sandstones to plot near the  $Fe_T O_3 + MgO$  apex evidently reflects winnowing and concentration of heavy minerals as well as destruction of feldspar.

The set of Eocene sandstone analyses offers an opportunity to explore an alternative means of chemical classification, using trace elements instead of major oxides. Trace element values are commonly subject to cutoff at the lower limit of analytical detection so that, for computational purposes, values for samples falling below the limit must be arbitrarily set at a fraction of the limiting value. For the trace elements Co and Ga, discussed below, the lower limits of detection were 8 and 10 ppm, respectively. For averaging values at localities, 2 ppm was substituted for  $< 8$  ppm Co and 5 ppm was substituted for  $< 10$  ppm Ga (Vine and Tourtelot, 1973, tab. 6).

Among locality averages for Eocene sandstones, trace elements showing a high correlation with  $\log(SiO_2/Al_2O_3)$  are Ba and Ga, with log Ga having the highest (negative) correlation of -0.86 (Fig. 8A). Gallium may be expected to substitute for Al in feldspar, and thus reflects feldspar content. Trace elements showing a high correlation with  $\log((Fe_T O_3 + MgO)/(K_2O + Na_2O))$  are Co, Cr, and Ni, with log Co showing the highest (0.61) correlation (Fig. 8B). Cobalt (as well as other heavy metals) occurs in magnetite and ilmenite, as can be verified by spectrographic analysis of magnetic concentrates (Lovering and Heddal, 1987). Absent grains of mineralized or mafic rock, Co reflects the abundance of magnetite and ilmenite. No trace elements are highly correlated with  $\log(K_2O/Na_2O)$ . Log Ga and log Co were selected as proxies for  $\log(SiO_2/Al_2O_3)$  and  $\log((Fe_T O_3 + MgO)/(K_2O + Na_2O))$ , respectively, to test classification by trace element content.

A scattergram of log Co vs log Ga identifies arkosic Eocene sandstone localities effectively (Fig. 9). As with diagrams of major oxide ratios, arkose localities plot slightly below and to the right of subarkose localities. Subarkose tends to plot close to the line separating arkosic sandstone from quartzose sandstone.

Both major-oxide and trace element scattergrams of Eocene sandstones reflect the high feldspar (especially potassium feldspar) and low iron oxide (probably, magnetite and ilmenite) content of arkose relative to quartzose sandstone. This relationship, seen also in major

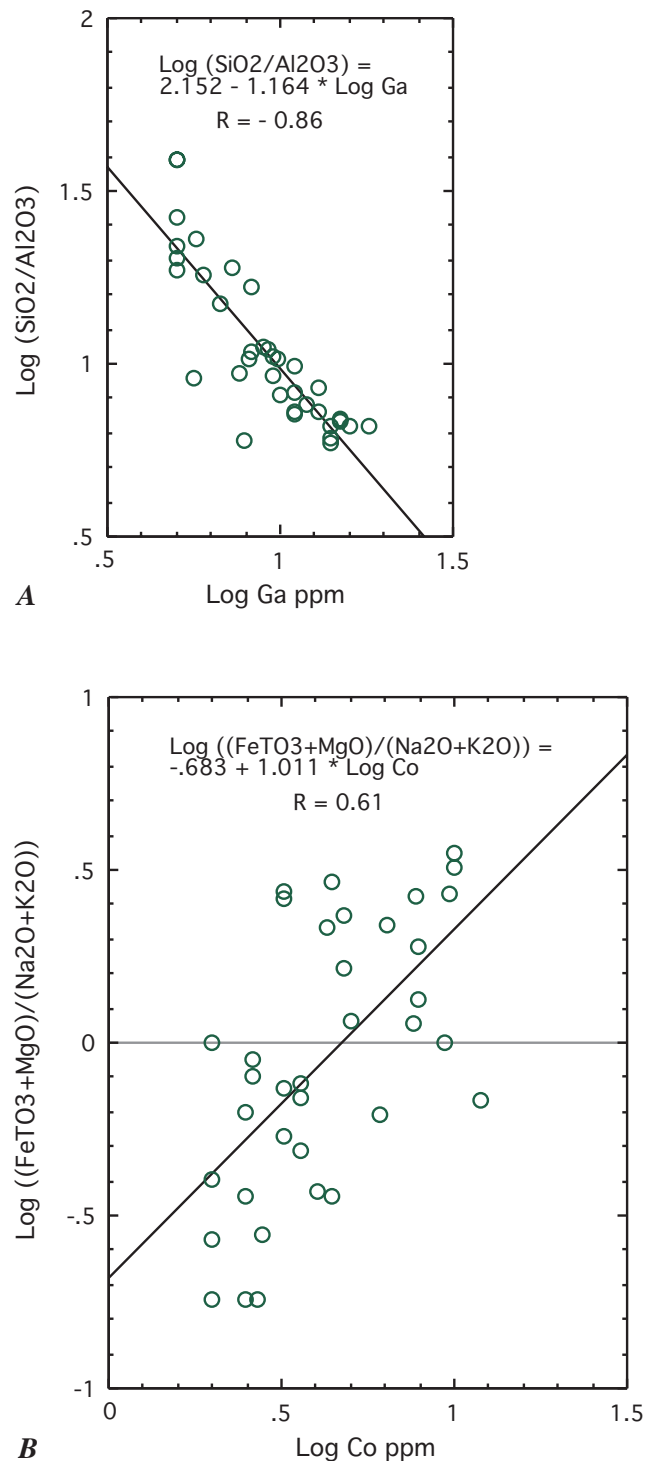
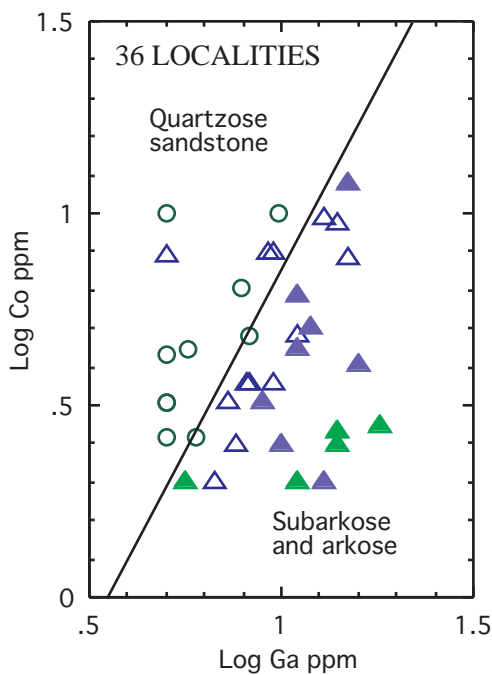


**Figure 8.**—Scattergrams showing correlations of A)  $\log(SiO_2/Al_2O_3)$  vs  $\log Ga$  ppm and B)  $\log((Fe_T O_3 + MgO)/(K_2O + Na_2O))$  vs  $\log Co$  ppm, average values for Eocene sandstones at 36 localities in Rocky Mountain foreland basins, western United States.



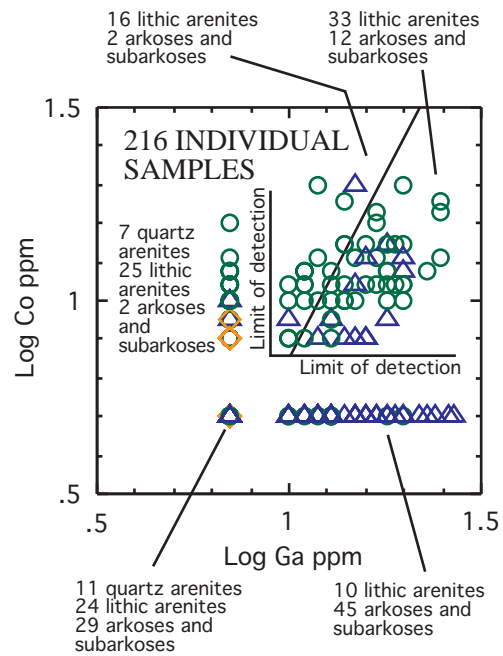
EXPLANATION

- Quartzose sandstone (< 10 pct feldspar)
- △ Subarkose (10-25 pct feldspar)
- ▲ Arkose (> 25 pct feldspar)
- ▲ Arkose (> 25 pct feldspar) near Granite Mountains

**Figure 9.**—Scattergram of log Co ppm vs log Ga ppm, average values for Eocene sandstones at 36 localities in Rocky Mountain foreland basins, western United States (data from Vine and Tourtelot, 1973). Localities are classified as in fig. 7, using mineral composition data of Vine and Tourtelot (1973).

oxide ratios of Pettijohn's (1963; 1975) tabulated analyses of sandstones, can probably be applied in other cases to separate feldspathic sandstone from quartzose sandstone.

As a follow-up experiment, all 216 individual chemically analyzed samples of Rocky Mountain Eocene sandstones were sorted into three classes using the major-oxide guidelines proposed at the end of the section on classification. These guidelines were used because mineralogic classification of individual samples was not available. Eighteen Eocene sandstones have  $\log(\text{SiO}_2/\text{Al}_2\text{O}_3) \geq 1.5$  and are considered to be quartz arenites. Ninety sandstones have  $\log(\text{SiO}_2/\text{Al}_2\text{O}_3) < 1.5$  and  $\log(\text{K}_2\text{O}/\text{Na}_2\text{O}) \geq 0$  and  $\log((\text{Fe}_T\text{O}_3 + \text{MgO})/(\text{K}_2\text{O} + \text{Na}_2\text{O})) < 0$ ; these are almost surely arkoses or subarkoses. The remaining 108 sandstones most resemble lithic arenites, having  $\log(\text{SiO}_2/\text{Al}_2\text{O}_3) < 1.5$  and either  $\log(\text{K}_2\text{O}/\text{Na}_2\text{O}) < 0$  or  $\log((\text{Fe}_T\text{O}_3 + \text{MgO})/(\text{K}_2\text{O} + \text{Na}_2\text{O})) \geq 0$ . Thirty-one of the samples classed as lithic arenites have  $\log(\text{K}_2\text{O}/\text{Na}_2\text{O}) < 0$  and thus could be confused with graywackes.



EXPLANATION

- ◇ Quartz arenite
- △ Arkose or subarkose
- Lithic arenite

**Figure 10.**—Scattergram of log Co ppm vs log Ga ppm for 216 samples of Eocene sandstone in Rocky Mountain foreland basins, western United States. Samples are classified using major oxide guidelines (see text). Samples plotted in lower left of diagram are below limit of analytical detection for both Co and Ga.

However, their continental fluvial depositional setting virtually rules out classification as true graywackes. Some of these sandstones may contain abundant clay matrix, however, and warrant the application of Gilbert's (Williams and others, 1954) term "wacke."

Finally, classification using only trace elements Co and Ga yielded a division of chemically defined quartz arenites from arkoses and subarkoses (Fig. 10), but no reliable identification of chemically defined lithic arenite. Only four arkoses and subarkoses defined by major oxide ratios were classified incorrectly as quartz arenite by log Co vs log Ga; 57 arkoses and subarkoses were classified correctly. No quartz arenites were misclassified. Lithic arenites defined by major oxide ratios were classified on both sides of the log Co vs log Ga line separating quartz arenites from arkoses and subarkoses. Thus, Co and Ga cannot be used to identify lithic arenites. Also, a large number (64) of samples have values below the limit of analytical detection for both Co and Ga, thus prohibiting

any classification. The failure to classify almost 30 pct of the samples emphasizes the importance of precision and low detection limits for classification by trace elements.

#### COMPOSITION OF MIDCONTINENT PENNSYLVANIAN

##### LITHIC ARENITES AND CLAY-RICH SANDSTONES

Quartz-clay sandstones that chemically resemble lithic arenites dominate Pennsylvanian sandstones of eastern Kansas, Missouri, and northeastern Oklahoma. They are discussed here to explore the chemical similarity of quartz-clay mixtures and petrographically-defined lithic arenites.

The Pennsylvanian Midcontinent sandstones were deposited in fluvial and coastal marine environments that developed during low sea level stands. During high sea level much of middle North America, north of the Ouachita orogenic belt, and from the Ancestral Rocky Mountains to the Appalachian orogenic belt, was covered by a vast epicontinental sea (McKee and Crosby, 1975). Most of the sandstones fill incised alluvial channels at the base of cyclic marine sequences of limestone and shale (Elias, 1964). The well-studied Bluejacket Sandstone Member of the Desmoinesian Boggy Formation records a southward-flowing incised stream in eastern Kansas that ends in a coastal delta in northeastern Oklahoma (Visher, in Shelton, 1973). Channels of the Tonganoxie Sandstone Member of the Virgilian Stranger Formation (not represented among the samples) likewise flowed southward into a delta in southeastern Kansas (Walton and Griffith, 1985). Although paleogeographic reconstructions for many of the sandstones are incomplete, most were probably derived from low-lying sources north of the Midcontinent Pennsylvanian sea or, like the channel sandstones of the Missourian Pleasanton Group (Elias, 1964), from the locally emergent Ozark uplift.

A total of 32 sandstone samples were collected from four complete sections of the Pennsylvanian System in northwestern Missouri and northeastern Kansas (hereafter referenced as the "northern area") and in northeastern Oklahoma (hereafter referenced as the "southern area") (Connor and Ebens, 1980). The northern area is interpreted to represent mostly fluvial channel sandstones located nearest to their source; the southern area is interpreted to represent mostly fluvial deltaic sandstones, some of which have been reworked by marine currents. Each sample was analyzed for major and trace elements (Boerngen and others, 1975). Splits of seven samples were analyzed at the same time, so that the data set contains a total of 39 analyses. All 39 analyses were retained for the present investigation.

No modal analyses of the samples are available, but the normative mineralogy has been described as a mixture of quartz and clay (Connor and Ebens, 1980). Among the sandstones represented in this data set, those of the Virgilian Wabaunsee Group in Kansas (Mudge and Yochelson, 1962), the Virgilian Lawrence Shale in Kansas (Sanders, 1959), the Pleasanton Group (Singler, 1965), and

the Bluejacket Sandstone Member in northeastern Oklahoma (Shelton, 1973) are most commonly described as quartz-rich, silty or clayey, micaceous, and containing clasts of shale and limestone. Desmoinesian sandstones of northeastern Oklahoma (including the Bluejacket Sandstone Member, Senora Formation, and sandstones associated with the Labette Shale, all represented in the data set) are mostly quartz and lithic arenites (Dyman, 1989). In the classification system of Blatt and others (1972), all analyses plot in or near the field of ferromagnesian potassic sandstones (Fig. 11D), comparable to lithic arenites (compare with Fig. 2B).

Major oxide ratios of the Pennsylvanian sandstones are consistent with classification as lithic arenite (Figs. 11A,B). Although twelve analyses have < 5 pct  $Al_2O_3$ , most do not chemically resemble quartz arenite. Based on proposed guidelines for use of major oxide ratios to classify sandstones, five analyses are consistent with quartz arenites [ $\log (SiO_2/Al_2O_3) \geq 1.5$ ], four analyses are consistent with arkoses or subarkoses [ $\log (SiO_2/Al_2O_3) < 1.5$  and  $\log (K_2O/Na_2O) \geq 0$  and  $\log ((Fe_T O_3 + MgO)/(K_2O + Na_2O)) < 0$ ], and the remaining 30 analyses most resemble lithic arenites [ $\log (SiO_2/Al_2O_3) < 1.5$  and either  $\log (K_2O/Na_2O) < 0$  or  $\log ((Fe_T O_3 + MgO)/(K_2O + Na_2O)) \geq 0$ ]. The lithic arenite classification probably results not so much from contained lithic grains as the effect of clay matrix and intraclasts on chemical composition.

Indications of major amounts of cement are limited to three analyses with abundant carbonate and three more with moderate carbonate; none are high in MgO (dolomitic). Thus inclusion of MgO in ratios should not present problems in classification or interpretation. One sample contains 11 pct  $Fe_T O_3$ , probably as hematite cement.

The distribution of analyses in the classification system of Herron (1988) is noteworthy (Fig. 11C). Only 18 of 39 analyses fall in the lithic arenite (litharenite and sublitharenite) field; most of the other analyses are in the fields of wackes and iron-rich sediments. While such classification may be explained by the chemical composition of these sandstones (for example, high  $Fe_T O_3$  vs  $K_2O$  of some), it does not correspond to any plausible petrographic classification (e.g., Dyman, 1989).

All of the analyses of samples from the northern area (Kansas and Missouri) closely resemble one another chemically (Fig. 11A,B); they are best classified as chemical lithic arenites, or simply clay-rich sandstone. The origin of the clay is unknown; it may be detrital, diagenetic, or both. In contrast to sandstones of the northern area, sandstones from the southern area are chemically diverse; many have lower  $K_2O/Na_2O$ , others have higher  $K_2O/Na_2O$ , and still others are silica-rich quartz arenites. Chemical diversity is also apparent among southern sandstones of the Wabaunsee Group, which is present in both areas. The chemical diversity of Pennsylvanian sandstones in the southern area may reflect reworking and sorting by marine currents, variable

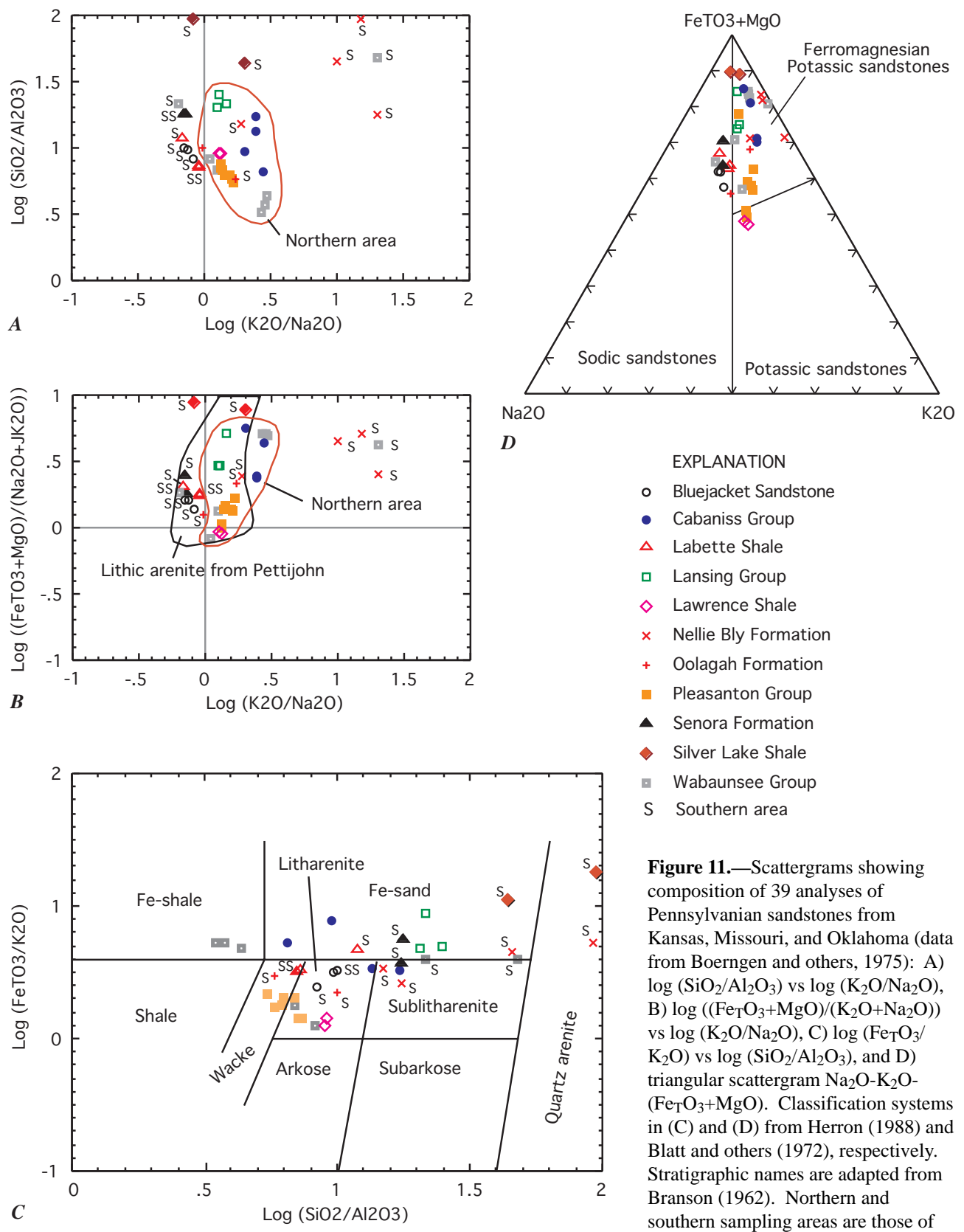


**Figure 11.**—Scattergrams showing composition of 39 analyses of Pennsylvanian sandstones from Kansas, Missouri, and Oklahoma (data from Boerngen and others, 1975): A)  $\log (\text{SiO}_2/\text{Al}_2\text{O}_3)$  vs  $\log (\text{K}_2\text{O}/\text{Na}_2\text{O})$ , B)  $\log ((\text{Fe}_T\text{O}_3+\text{MgO})/(\text{K}_2\text{O}+\text{Na}_2\text{O}))$  vs  $\log (\text{K}_2\text{O}/\text{Na}_2\text{O})$ , C)  $\log (\text{Fe}_T\text{O}_3/\text{K}_2\text{O})$  vs  $\log (\text{SiO}_2/\text{Al}_2\text{O}_3)$ , and D) triangular scattergram  $\text{Na}_2\text{O}-\text{K}_2\text{O}-(\text{Fe}_T\text{O}_3+\text{MgO})$ . Classification systems in (C) and (D) from Herron (1988) and Blatt and others (1972), respectively. Stratigraphic names are adapted from Branson (1962). Northern and southern sampling areas are those of Connor and Ebens (1980).

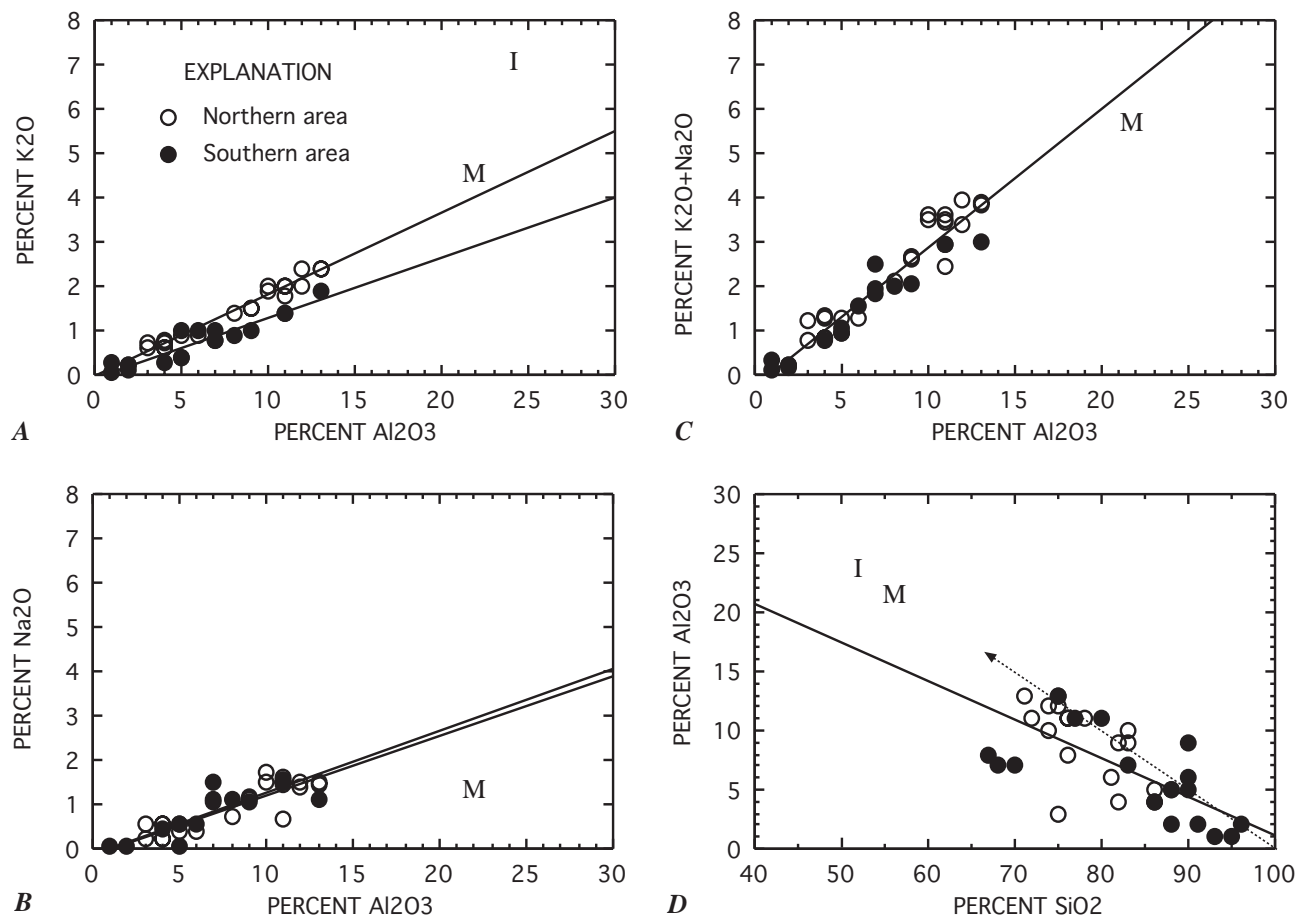


**Figure 12.**—Variation scattergrams of 39 analyses of Pennsylvanian sandstones from Kansas, Missouri, and Oklahoma (data from Boerngen and others, 1975): A)  $K_2O$  vs  $Al_2O_3$ , B)  $Na_2O$  vs  $Al_2O_3$ , C)  $K_2O+Na_2O$  vs  $Al_2O_3$ , and D)  $Al_2O_3$  vs  $SiO_2$ . All values in weight percent, uncorrected for volatile components. Three samples with abundant calcite cement not plotted in (D). I, average illite (Weaver and Pollard, 1973, tab. I), M, mixed layer illite- smectite (68 pct illite, Newman and Brown, 1987, tab. 1-31, analysis 5). Solid lines show best fit by linear regression; two lines, separate fit for northern and southern areas; one line, areas combined. Dashed line in (D) is possible mixing line.

provenance (Dyman, 1989), or both. Redistribution of sand by marine currents has been inferred from reconstruction of the delta of the Bluejacket Sandstone Member (Shelton, 1973).

An experiment was conducted to see if the composition of the Midcontinent Pennsylvanian sandstones could be explained by quartz-clay mixing (Fig. 12), following the method described by Argast and Donnelly (1987). Potash,  $Na_2O$ , and  $K_2O+Na_2O$  are all highly correlated with  $Al_2O_3$  (Figs. 12A,B,C); fitted lines extend to the origin, suggesting that the content of these oxides could be explained by mixing two components. Alumina and  $SiO_2$  are also correlated (negatively), but less so (Fig. 12D). The composition of average illite is well above the line for  $K_2O$  vs  $Al_2O_3$  (Fig. 12A), indicating that  $K_2O$  content is too small to account for the observed covariation by mixing quartz and illite. The composition of mixed layer illite-smectite varies widely (e.g., Newman and Brown, 1987), but mixing with quartz allows  $Na_2O$  as well as  $K_2O$  to covary with  $Al_2O_3$  (Fig. 12B). If

$K_2O+Na_2O$  is plotted against  $Al_2O_3$ , an illite-smectite clay composition can be found that will plot close to the mixing line (Fig. 12C). Mixing of feldspar, with  $K_2O$  and  $Na_2O$  that plot well above the mixing lines and off the diagrams in Figs. 12A,B, and C, cannot explain the observed well-defined correlations. Most of the Pennsylvanian sandstones of northeastern Oklahoma are feldspar-poor (Dyman, 1989). Thus, the chemical composition of Midcontinent Pennsylvanian sandstones is consistent with that obtained from mixing variable amounts of quartz and illite-smectite clay. Noncarbonate lithic fragments in the sandstones are likewise quartz (chert) and clay (shale), or mixtures of the two.

Normative mineral calculations (method of Cohen and Ward, 1991) suggest that mixtures composed principally of quartz, illite, and smectite (equivalent to quartz and illite-smectite) make up the mineral composition of Midcontinent Pennsylvanian sandstones. An analysis of sandstone from the Pleasanton Group, which is among those having low  $\log(SiO_2/Al_2O_3)$ , and therefore most



likely to contain clay or feldspar (Fig. 11A), was selected for normative mineral calculations. Using varying assumptions to allocate potassium to feldspar and illite, and Ca, Na, Fe, and Mg to smectite, the sandstone has a normative mineral content of about 50 weight pct quartz, 0-8 pct potassium feldspar (8 pct is probably unrealistically high), 10-20 pct illite, possibly as much as two pct kaolinite, 20-30 pct smectite, and < 4 pct cement and accessory minerals.

### CONCLUSIONS

The major classes of sandstones can be defined by their chemical composition, albeit with varying degrees of certainty ranging from high (for quartz arenite), moderate (for graywacke and arkose) to low (for lithic arenite). Scattergrams of major oxide ratios transformed to logarithms appear to be the most useful for separating sandstone classes. The ratios  $\text{SiO}_2/\text{Al}_2\text{O}_3$ ,  $\text{K}_2\text{O}/\text{Na}_2\text{O}$ , and  $(\text{Fe}_T\text{O}_3+\text{MgO})/(\text{Na}_2\text{O}+\text{K}_2\text{O})$  reflect processes of sandstone formation and are amenable to process interpretation. Compositional fields can be defined on scattergrams, but are known with varying degrees of certainty for each class. General guidelines for classification, proposed in this report, offer a point of departure for classification and further study. Understanding how a population of sandstones acquired its chemical attributes can be enhanced by identifying mixing lines, formed when varying amounts of two or more minerals cause well-defined correlations among minerals and major oxides. Trace elements, notably gallium and cobalt, may also be used to classify sandstones, but considerable work remains to establish their reliability.

The various chemical classification systems compared here yield somewhat disparate results, but their use together can enhance the likelihood of correctly classifying individual sandstones. Disparate classification of individual sandstones is an indicator that further study is required to understand their true identity and origin. All classification systems and guidelines should be used with caution because of the complex effects of mineral content on bulk chemical composition.

### Acknowledgements

This work relies heavily on the efforts of others, who painstakingly acquired and compiled chemical analyses of sandstones. Although they are cited in the text and references, I here acknowledge a special debt to J. D. Vine and E. B. Tourtelot, whose data set on Rocky Mountain Eocene sandstones was particularly useful in testing various approaches to the classification of arkosic sandstones, and J. J. Connor and R. J. Ebens, whose data set on Midcontinent Pennsylvanian sandstones provided an insightful example of the challenges posed in understanding the chemical composition of lithic arenites. Equally worthy of mention is the contribution of the many chemists of the U. S. Geological Survey who generated the above-mentioned data sets; they are listed in the

referenced data sources. I thank T. S. Dyman, U. S. Geological Survey, and M. M. Herron, Schlumberger-Doll Research, for comments on earlier versions of the manuscript. Finally, I make special mention of the late F. J. Pettijohn, who long ago encouraged my interest in sedimentary rocks, and whose work laid some of the foundation for chemical investigation of sandstones.

### References cited

- Argast, S., and Donnelly, T. W., 1987, The chemical discrimination of clastic sedimentary components: *Journal of Sedimentary Petrology*, v. 57, no. 5, p. 813-823.
- Bhatia, M. R., 1983, Plate tectonics and geochemical composition of sandstones: *Journal of Geology*, v. 91, no. 6, p. 611-627.
- Blatt, H., Middleton, G., and Murray, R., 1972, *Origin of sedimentary rocks*: Englewood Cliffs, New Jersey, Prentice-Hall, 634 p.
- Boerngen, J. G., Van Trump, G., Jr., and Ebens, R. J., 1975, Analytical data for geologic units in Missouri and parts of Kansas, Oklahoma, and Arkansas: U. S. Geological Survey Open-file Report 75-137, 276 p.
- Branson, C. C., 1962, Pennsylvanian system of the midcontinent, *in* Branson, C. C., ed., *Pennsylvanian system in the United States—a symposium*: Tulsa, American Association of Petroleum Geologists, p. 431-460.
- Chayes, F., 1960, On correlation between variables of constant sum: *Journal of Geophysical Research*, v. 65, no. 12, p. 4185-4193.
- Cohen, D., and Ward, C. R., 1991, SEDNORM—a program to calculate a normative mineralogy for sedimentary rocks based on chemical analyses: *Computers and Geosciences*, v. 17, no. 9, p. 1235-1253.
- Connor, J. J., 1969, A geochemical discriminant for sandstones of Mississippian and Pennsylvanian age in Kentucky: *Colorado School of Mines Quarterly*, v. 64, no. 3, p. 17-34.
- Connor, J. J., and Ebens, R. J., 1980, Geochemistry of bedrock units in Missouri and parts of adjacent states: U. S. Geological Survey Professional Paper 954-F, 55 p.
- Crook, K. A. W., 1974, Lithogenesis and geotectonics: the significance of compositional variation in flysch arenites (graywackes), *in* Dott, R. H., Jr., and Shaver, R. H., eds., *Modern and ancient geosynclinal sedimentation*: Society of Economic Paleontologists and Mineralogists Special Publication No. 19, p. 304-310.
- Cummins, W. A., 1962, The graywacke problem: *Liverpool Manchester Geological Journal*, v. 3, pt. 1, p. 51-72.
- Dickinson, W. R., Klute, M. A., Hayes, M. J., Janecke, S. U., Lundin, E. R., McKittrick, M. A., and Olivares, M. D., 1988, Paleogeographic and paleotectonic setting



- of Laramide sedimentary basins in the central Rocky Mountain region: Geological Society of America Bulletin, v. 100, no. 7, p. 1023-1039.
- Dyman, T. S., 1989, Statistical analysis of compositional data from Desmoinesian sandstones in Oklahoma: U. S. Geological Survey Bulletin 1866-B, 12 p.
- Ehrenberg, S. N., and Siring, E., 1992, Use of bulk chemical analyses in stratigraphic correlation of sandstones: an example from the Statfjord Nord field, Norwegian continental shelf: Journal of Sedimentary Petrology, v. 62, no. 2, p. 318-330.
- Elias, M. K., 1964, Depth of late Paleozoic sea in Kansas and its megacyclic sedimentation, *in* Merriam, D. F., ed., Symposium on cyclic sedimentation: Kansas Geological Survey Bulletin 169, v. 1, p. 87-106.
- Fedo, C. M., Nesbitt, H. W., and Young, G. M., 1995, Unraveling the effects of potassium metasomatism in sedimentary rocks and paleosols, with implications for paleoweathering conditions and provenance: Geology, v. 23, no. 10, p. 921-924.
- Floyd, P. A., Shail, R., Leveridge, B. E., Franke, W., 1991, Geochemistry and provenance of Rhenohercynian synorogenic sandstones: implications for tectonic environment discrimination, *in* Morton, A. C., Todd, S. P., Haughton, P. D. W., eds., Developments in Sedimentary Provenance Studies: Geological Society of London Special Publication No. 57, p. 173-188.
- Herron, M. M., 1988, Geochemical classification of terrigenous sands and shales from core or log data: Journal of Sedimentary Petrology, v. 58, no.5, p. 820-829.
- Herron, S. L., and Herron, M. M., 1996, Quantitative lithology: an application for open and cased hole spectroscopy: Transactions of the SPWLA 37th Annual Logging Symposium, New Orleans, LA, June 16-19, 1996, Paper E, 14 p.
- Herron, M. M., and Matteson, A., 1993, Elemental composition and nuclear parameters of some common sedimentary minerals: Nuclear Geophysics, v. 7, no. 3, p. 383-406.
- Hickman, A. H., and Wright, A. E., 1983, Geochemistry and chemostratigraphical correlation of slates, marbles, and quartzites of the Appin Group, Argyll, Scotland: Transactions of the Royal Society of Edinburgh: Earth Sciences, v. 73, p. 251-278.
- Hubert, J. F., Feshbach-Meriney, P. E., and Smith, M. A., 1992, The Triassic-Jurassic Hartford rift basin, Connecticut and Massachusetts: evolution, sandstone diagenesis, and hydrocarbon history: American Association of Petroleum Geologists Bulletin, v. 76, no. 11, p. 1710-1734.
- Huckenholz, H. G., 1963, Mineral composition and texture in graywackes from the Harz Mountains (Germany) and in arkoses from the Auvergne (France): Journal of Sedimentary Petrology, v. 33, no. 4, p. 914-918.
- Humphreys, B., Morton, A. C., Hallsworth, C. R., Gatliff, R. W., Riding, J. B., 1991, An integrated approach to provenance studies: a case example from the Upper Jurassic of the Central Graben, North Sea, *in* Morton, A. C., Todd, S. P., Haughton, P. D. W., eds., Developments in Sedimentary Provenance Studies: Geological Society of London Special Publication No. 57, p. 251-262.
- Kuenen, Ph. H., 1966, Matrix of turbidites: an experimental approach: Sedimentology, v. 7, p. 267-297.
- Le Maitre, R. W., 1976, The chemical variability of some common igneous rocks: Journal of Petrology, v. 17, no. 4, p. 589-637.
- Lindsey, D. A., 1972, Sedimentary petrology and paleocurrents of the Harebell Formation, Pinyon Conglomerate, and associated coarse clastic deposits, northwestern Wyoming: U. S. Geological Survey Professional Paper 734-B, 68 p.
- Love, J. D., 1970, Cenozoic geology of the Granite Mountains area, central Wyoming: U. S. Geological Survey Professional Paper 495-C, 154 p.
- Lovering, T. G., and Hedall, J. A., 1987, Trace elements in magnetic concentrates from stream sediments in southwestern New Mexico—a potential tool for reconnaissance geochemical exploration in arid lands: U. S. Geological Survey Bulletin 1566, 31 p.
- McCann, T., 1991, Petrological and geochemical determination of provenance in the southern Welsh Basin, *in* Morton, A. C., Todd, S. P., Haughton, P. D. W., eds., Developments in Sedimentary Provenance Studies: Geological Society of London Special Publication No. 57, p. 215-230.
- McLennan, S. M., Hemming, S., McDaniel, D. K., and Hanson, G. N., 1993, Geochemical approaches to sedimentation, provenance, and tectonics, *in* Johnson, M. J., and Basu, A., eds., Processes controlling the composition of clastic sediments: Geological Society of America Special Paper 284, p. 21-40.
- McKee, E. D., and Crosby, E. J., coordinators, 1975, Paleotectonic investigations of the Pennsylvanian system in the United States: U.S. Geological Survey Professional Paper 853, 3 parts, 17 plates.
- Miesch, A. T., Chao, E. C. T., and Cuttitta, F., 1966, Multivariate analysis of geochemical data on tektites: Journal of Geology, v. 74, no. 5, pt. 2, p. 673-691.
- Middleton, G. V., 1960, Chemical composition of sandstones: Geological Society of America Bulletin, v. 71, no. 7, p. 1011-1026.
- Middleton, G. V., 1972, Albite of secondary origin in Charny sandstones, Quebec: Journal of Sedimentary Petrology, v. 42, no. 2, p. 341-349.
- Mudge, M. R., and Yochelson, E. L., 1962, Stratigraphy and paleontology of the uppermost Pennsylvanian and lowermost Permian rocks in Kansas: U. S. Geological Survey Professional Paper 323, 213 p.
- Newman, A. C. D., and Brown, G., 1987, The chemical constitution of clays, *in* Newman, A. C. D., ed.,

- Chemistry of clays and clay minerals, Mineralogical Society Monograph No. 6: New York, Wiley, p. 1-128.
- Pettijohn, F. J., 1963, Chemical composition of sandstones—excluding carbonate and volcanic sands, *in* Fleischer, M., ed., Data of Geochemistry, sixth edition, U. S. Geological Survey Professional Paper 440-S, 21 p.
- Pettijohn, F. J., 1975, Sedimentary rocks, third edition: New York, Harper & Row, 628 p.
- Pettijohn, F. J., Potter, P. E., and Siever, R., 1972, Sand and sandstone: New York, Springer, 618 p.
- Potter, P. E., 1978, Petrology and chemistry of modern big river sands: *Journal of Geology*, v. 86, no. 4, p. 423-449.
- Roehler, H. W., 1993, Eocene climates, depositional environments, and geography, greater Green River basin, Wyoming, Utah, and Colorado: U. S. Geological Survey Professional Paper 1506-F, 74 p.
- Roser, B. P., and Korsch, R. J., 1986, Determination of tectonic setting of sandstone-mudstone suites using SiO<sub>2</sub> content and K<sub>2</sub>O/Na<sub>2</sub>O ratio: *Journal of Geology*, v. 94, no. 5, p. 635-650.
- Roser, B. P., and Korsch, R. J., 1988, Provenance signatures of sandstone-mudstone suites determined using discriminant function analysis of major-element data: *Chemical Geology*, v. 67, no. 1, p. 119-139.
- Sanders, D. T., 1959, Sandstones of the Douglas and Pedee Groups in northeastern Kansas: *Kansas Geological Survey Bulletin* 134, pt. 3, p. 125-159.
- Schwab, F. L., 1975, Framework mineralogy and chemical composition of continental margin-type sandstone: *Geology*, v. 3, no. 9, p. 487-490.
- Singler, C. R., 1965, Preliminary remarks on the stratigraphy of the Pleasanton Group (Pennsylvanian) in the northern Midcontinent: *The Compass*, v. 42, no. 2, p. 63-72.
- Shelton, J. W., 1973, Models of sand and sandstone deposits: a methodology for determining sand genesis and trend: *Oklahoma Geological Survey Bulletin* 118, 122 p.
- Utada, M., and Vine, J. D., 1984, Zonal distribution of zeolites and authigenic plagioclase, Spanish Peaks region, southern Colorado: *in* Olson, D., and Bislo, A., eds., Proceedings, Sixth International Zeolite Conference, London, Butterworths, p. 604-615.
- Vine, J. D., and Tourtelot, E. B., 1973, Geochemistry of Lower Eocene sandstones in the Rocky Mountain Region, with a section on direct-reader spectrometric analyses, by R. G. Havens and A. T. Myers: U. S. Geological Survey Professional Paper 789, 36 p.
- Walker, T. R., 1967, Formation of red beds in modern and ancient deserts: *Geological Society of America Bulletin*, v. 78, no. 3, p. 353-368.
- Walton, A. W., and Griffith, G., 1985, Deltaic deposition in the Tonganoxie or "Stalnaker" Sandstone (Stranger Formation, Virgilian): TXO Robinson C-1, Harper County, Kansas, *in* Watney, W. L., Walton, A. W., and Doveton, J. H., comps., Core studies in Kansas: *Kansas Geological Survey Subsurface Geology Series* 6, p. 145-160.
- Weaver, C. E., and Pollard, L. D., 1973, The chemistry of clay minerals, *Developments in Sedimentology* 15: Amsterdam, Elsevier, 213 p.
- Williams, H., Turner, F. J., and Gilbert, C. M., 1954, Petrography: an introduction to the study of rocks in thin sections: San Francisco, Freeman, 406 p.
- Young, G. M., and Nesbitt, H. W., 1998, Processes controlling the distribution of Ti and Al in weathering profiles, siliciclastic sediments and sedimentary rocks: *Journal of Sedimentary Research*, v. 68, no. 3, p. 448-455.